Description of a novel extremophile green algae, *Chlamydomonas pacifica*, and its potential as a biotechnology host

João Vitor Dutra Molino[1], Aaron Oliver[2], Harish Sethuram[3], Kalisa Kang[1], Barbara Saucedo[1], Crisandra Jade Diaz[1], Abhishek Gupta[1,4], Lee Jong Jen[1,11], Yasin Torres-tiji[1,5], Nora Hidasi[1,6], Amr Badary[1,7,8], Hunter Jenkins[1,10], Francis J. Fields[1,10], Stephen Mayfield[1,9,10,*]

[1] Department of Molecular Biology, School of Biological Sciences, University of California San Diego, San Diego, CA, United States.

[2] Center for Marine Biotechnology and Biomedicine, Scripps Institution of Oceanography, University of California San Diego, La Jolla, CA, United States.

[3] Infectious Disease and Microbiome Program, Broad Institute of MIT and Harvard, Cambridge, MA, USA.

[4] Microbial and Environmental Genomics Department, J. Craig Venter Institute, La Jolla, CA, USA.

[5] Colorado School of Mines, Golden, CO, USA

[6] Department of Biology and Biotechnologies "Charles Darwin", Sapienza University of Rome, Piazzale Aldo Moro, 5, 00185, Rome, Italy

[7] Division of Pulmonary Diseases and Critical Care Medicine, University of California, Irvine, CA, United States

[8] UCI Sleep Disorders Center, University of California, Irvine, 20350 Birch St., Newport Beach, CA, 92660, USA

[9] Algenesis Inc., 1238 Sea Village Dr., Cardiff, CA, USA.

[10] California Center for Algae Biotechnology, University of California, San Diego, La Jolla, CA, United States.

[11] Sarawak Biodiversity Centre, KM20, Jalan Puncak Borneo, 93250 Kuching, Sarawak, Malaysia.

* Correspondence: Stephen Mayfield (smayfield@ucsd.edu)

ORCIDs

João Vitor Dutra Molino: https://orcid.org/0000-0003-2475-9807

Aaron Oliver: https://orcid.org/0000-0002-0410-8284

Harish Sethuram: https://orcid.org/0000-0001-6061-9575

Kalisa Kang: https://orcid.org/0009-0006-1939-8129

Barbara Saucedo: https://orcid.org/0009-0000-0886-0839

Crisandra Jade Diaz: https://orcid.org/0000-0001-7342-9041

Abhishek Gupta: https://orcid.org/0000-0003-0136-3340

Lee Jong Jen: https://orcid.org/0000-0001-7168-2510

Yasin Torres-tiji: https://orcid.org/0000-0001-8976-1620

Nora Hidasi: https://orcid.org/0000-0002-7554-768X

Amr Badary: https://orcid.org/0009-0009-4671-1426

Francis J. Fields: https://orcid.org/0000-0003-1152-2405

Stephen Mayfield: https://orcid.org/0000-0001-7642-9047

Keywords: biotechnology, microalgae, new species, extremophile, bioplastic.

Graphical Abstract

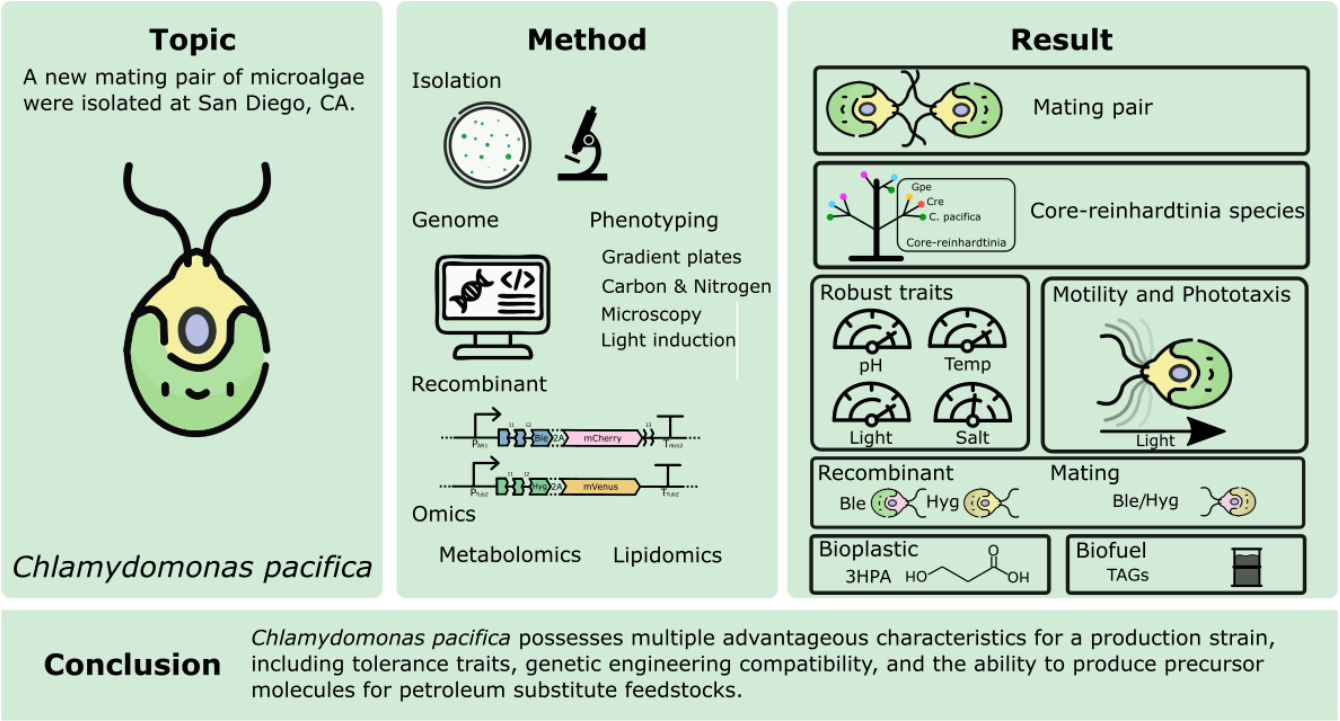

Icon made by Pixel perfect, Freepik and Uniconlabs from www.flaticon.com

Abstract

We present the comprehensive characterization of a newly identified microalga, *Chlamydomonas pacifica*, originally isolated from a soil sample in San Diego, CA, USA. This species showcases remarkable biological versatility, including a broad pH range tolerance (6-11.5), high thermal tolerance (up to 42°C), and salinity resilience (up to 2% NaCl). Its amenability to genetic manipulation and sexual reproduction via mating, particularly between the two opposing strains CC-5697 & CC-5699, now publicly available through the Chlamydomonas Resource Center, underscores its potential as a biotechnological chassis. The biological assessment of *C. pacifica*, revealed versatile metabolic capabilities, including diverse nitrogen assimilation capability, phototaxis, and motility. Genomic and transcriptomic analyses identified 17,829 genes within a 121 Mb genome, featuring a slightly lower GC content (61%) than the model organism *Chlamydomonas reinhardtii*. The codon usage of *C. pacifica* closely mirrors that of *C. reinhardtii*, indicating a conserved genetic architecture that supports a trend in codon preference with minor variations. Phylogenetic analyses position *C. pacifica* within the core-Reinhardtinia clade yet distinct from known Volvocales species. Through metabolomic and lipidomic profiling, we observed a high carbohydrate content, approximately 30% of the dry cell weight (DCW), suggesting a substantial capacity for bioplastic precursor production. The lipidomic data revealed an abundance of triacylglycerols (TAGs), promising for biofuel applications and lipids for health-related benefits. Our investigation lays the groundwork for exploiting *C. pacifica* in

biotechnological applications, spanning from biofuel generation to synthesizing biodegradable plastics, positioning it as a versatile host for future bioengineering endeavors.
.

Keywords: Chlorophyte, alkali tolerant, bioplastic precursors, mating capacity, stress tolerance (pH, temperature, salinity).

Introduction

Green algae are generally aquatic plant-like organisms found in various environments, including freshwater, marine, but also terrestrial habitats, and are the closest related species to land plants (Delwiche & Cooper, 2015). Their diversity is also reflected in the potential applications within biotechnology, where numerous species, including unicellular *Chlorela vulgaris*, *Dunaliela salina*, and *Chlamydomonas reinhardtii*, are currently employed (Kumar et al., 2020). Additionally, macroalgae such as *Ulva lactuca* and *Enteromorpha spp*., commonly used in East Asian cuisines, have gained some attention for their biotechnological potential (Ren et al., 2022). The global algae products market is estimated to be valued at USD 1.92 billion in 2024, and is projected to expand to USD 2.45 billion by 2029, reflecting a Compound Annual Growth Rate (CAGR) of 4.99% (TMR, 2016). This underscores the burgeoning significance of algae-based applications across various industries. However, the reliable cultivation and production of these diverse species requires specific growing techniques, with some species relying on specialized equipment, such as closed photobioreactors to prevent contamination of the cultures (Novoveská et al., 2023). While algal systems are increasingly employed on large scales, their natural diversity is significantly broader. For instance, the genus Chlamydomonas contains more than 450 species reported (Milo et al., 2010), yet only a handful of species are used on a commercial scale (Tran et al., 2019). This is due to the suitability of specific species for producing desired products, as applications like nutraceuticals or functional foods that can accommodate higher production costs (Diaz et al., 2023; Ejike et al., 2023; Udayan et al., 2023; Vishwakarma et al., 2023), while others require lower costs, such as wastewater treatment, biofuel, bioplastic production and animal feed (Abdelfattah et al., 2023).

One notable advantage of algae cultivation lies in its ability to thrive in diverse environments, including non-arable lands and wastewater treatment facilities, thereby avoiding competition with food crop cultivation (Ahmad & Ashraf, 2023). Another advantage this crop holds over traditional terrestrial plants is its remarkable ability to thrive in a variety of water sources, including seawater and brackish water, the latter being a largely untapped resource where conventional crops typically fail to flourish. For example, in the United States alone, there is more than 800 times the amount of water currently used yearly in the form of brackish water bodies (Stanton et al., 2017). The location of the main basins also coincides with regions characterized by non-arable land, such as Arizona, New Mexico, Utah,

Nevada, California, and parts of Colorado—all benefiting from high sunlight incidence, making them ideal for algae cultivation. To achieve industrial-scale production, it is essential to select strains that exhibit consistent growth and can thrive in challenging conditions, including high light incidences, elevated temperatures, and brackish water. These regions are often underutilized for traditional land use or pastureland and represent untapped potential for algae cultivation. The ability of a strain to flourish in such environments not only expands the geographic scope for algae cultivation but also provides a strategic advantage in resource utilization.

The cost associated with cultivating a species is inherently tied to its traits and growth requirements. While *C. reinhardtii* can be grown on an industrial scale, its production is typically accomplished within closed bioreactors using an organic carbon source such as acetic acid (Masi et al., 2023). These closed systems provide conditions conducive to growth that are otherwise unsuitable for open systems. Therefore, the algae strain selection plays a crucial role on choice and feasibility of production systems. Growing in extreme conditions, which prevents the risk of contamination, favors the use of cheaper and more scalable systems like the high-salinity green algae *D. salina*, capable of thriving in 85 g/L of salt (B. Zhang et al., 2023). This adaptability simplifies management efforts and helps lower production costs (Varshney et al., 2015). Extremophiles are found in various extreme environments, including hot springs, ice caps, high salt (*Dunaliella* sp.), and acidic mines and rivers (*C. acidophila*) or soda lakes (*Spirulina platensis*) (Brock, 1975; Luís et al., 2022; Melack, 1979; Oren, 2014; Remias et al., 2005; Selvaratnam et al., 2014). Special adaptations allow them to survive in harsh conditions, making them interesting organisms for bioprospecting. On one hand, extremophiles can serve as sources of valuable tools, such as Taq polymerase; on the other hand, their inherent ability to grow in extreme conditions simplifies culturing management. For instance, maintaining them in high-salt conditions can help prevent contamination and protect against predators, addressing a significant obstacle faced in the cultivation process (McGowen, 2019; Varshney et al., 2015).

This work presents a newly isolated green algae capable of growing in high pH, elevated temperatures, high light irradiance, and brackish water salinity levels. We isolated two mating types capable of sexual reproduction, which we genetically engineered with different expression vectors. We demonstrated the capacity of daughter cells to harbor inherited traits from both parents. To further characterize the strain, an omics approach was employed, followed by sequencing, assembling, and annotating its genome. We then constructed a phylogenetic tree using 1,519 chlorophyta genes and 42 available algae species to place *Chlamydomonas pacifica* on the Core-reinhardtinia, of which *C. reinhardtii* is a distinguished member (Manni et al., 2021). The closest species is *Chlamydomonas sp.* 3222, another *Chlamydomonas* strain isolated in the United Arab Emirates (Nelson et al., 2019). We compared both strains pH, salt, light and temperature tolerance, revealing similar patterns. To assess potential applications of this new alga species, lipidomic analysis was performed on the culture. The strain presented a diverse profile of lipids useful to biofuels and health related applications. Altogether, *C. pacifica* shows great promise as a platform for bioproducts, driving a sustainable bioeconomy.

Material and Methods

Isolation and Characterization

Water samples were collected from a pond in the Biology field station of UCSD (32° 53 '09"N, 117° 13' 48"W) and plated on High-Salt Media (HSM) media (**Supplementary Table 1a**). Colonies were repeatedly streaked on the same medium to obtain pure colonies as confirmed by a single morphology and size when examined directly using a light microscope. Throughout the year 2023, this region exhibits an average monthly air temperature fluctuating between 10°C and 25°C, alongside solar radiation averages that range from 128 W/m^2 to 291 W/m^2 monthly, according to the California Irrigation Management Information System (CIMIS). The opposing mating type strains were deposited at chlamydomonas collection under strain number CC-5697 (402) & CC-5699 (403). Throughout the text we maintained the names *C. pacifica* 402 for CC-5697 and *C. pacifica* 403 for CC-5699.

Growth Conditions

The cultures were grown in various media, all described in the Supplementary material, at 25-28 °C under constant illumination of 80 µmol photons/m^{2}s and agitation of 150 rpm, in 50mL cultures unless stated otherwise (**Supplementary Table 1a-d**). To obtain the growth curve 160 uL media inoculated with samples added in 96 well plates and read in the Infinite® M200 PRO plate reader (Tecan, Männedorf, Switzerland), from 6 biological replicates for each strain and condition studied. The cultures were grown at 30 °C under constant illumination of 80 µmol photons/m^{2}s at 800 rpm on a rotary microplate shaker.

Genomic DNA and RNA Extraction

Cells were grown in HSM media and spun down, flashed frozen in liquid nitrogen and sent frozen to UCDavis genome center. The DNA was sequenced in the Nanopore sequencer PromethION for long reads and in Illumina NovaSeq 6000 for short reads. The RNA samples were extracted from cells grown until stationary phase photosynthetically in HSM media, mixotrophically in Tris-Acetate-Phosphate (TAP) media, heterotrophically in TAP media, and photosynthetically in high salt on the D2-15 media supplemented with 15g/L of Na_2CO_3. The RNA was extracted by pelleting cells by centrifugation at 3,000 × g for 1 minute at 4°C. The pellet was then resuspended in 0.25 mL lysis buffer containing 50 mM Tris-HCl (pH 8.0), 200 mM NaCl, 20 mM EDTA, 2% SDS, and Proteinase K (0.5mg/L). The lysate was incubated at 70°C for 2 minutes to ensure thorough lysis and was then mixed with 2 mL of TRIzol reagent. The mixture was incubated at room temperature for 5 minutes, followed by adding 0.5 mL of chloroform, which was vigorously shaken for 15 seconds. After a 5-minute incubation at room temperature, the sample was centrifuged at 12,000 × g for 15 minutes at 4°C. The aqueous phase was carefully transferred to a new tube, and RNA was precipitated by adding 1 mL of isopropanol, followed by a 10-minute incubation at 4°C. The

RNA was pelleted by centrifugation at 12,000 × g for 10 minutes at 4°C, and the supernatant was discarded. The RNA pellet was washed by resuspension in 2 mL of 75% ethanol, briefly vortexed, and centrifuged at 7,500 × g for 5 minutes at 4°C. The supernatant was discarded, and the RNA pellet was air dry for 5–10 minutes. The RNA pellet was resuspended in 25 µL of RNase-free water, 3.5 µL of 10X DNase buffer, and 5 µL of DNase were added, and the sample was incubated at room temperature for 1–2 hours. Finally, 3 µL of EDTA was added to the RNA solution, and the mixture was incubated at 65°C for 10 minutes to inactivate the DNase. The RNA samples were submitted to the UCSD IGM Genomics Center.

Genome Sequencing and Annotation

Long DNA reads were produced using Oxford Nanopore sequencing on the PromethION platform. These long reads were cleaned, trimmed, and assembled with Flye version 2.9.3, using default program parameters except for an estimated genome size of 120m (Kolmogorov et al., 2019). This assembly produced 14 contigs longer than one million nucleotides, with an N50 of 484,211. To improve local mis-assemblies in the genome, Illumina sequencing was performed using the Illumina NovaSeq 6000 platform. These short reads were cleaned and trimmed using fastp version 0.23.1 with default parameters (Chen et al., 2018). Illumina reads were given as input to Pilon version 1.24, and all downstream analyses were performed on this polished genome (Walker et al., 2014).

Additional RNA sequencing was carried out from four samples using the Illumina NovaSeq 6000 platform to support gene model predictions. These transcriptomic reads were cleaned using fastp and then mapped to the genome using STAR version 2.7.4a (Dobin et al., 2013). Mapped transcriptomic reads, the AUGUSTUS model for *Chlamydomonas reinhardtii*, and the OrthoDB version 10 set of Viridiplantae proteins were given to Braker v. 3.0.6 to predict gene models (Gabriel et al., 2024; Hoff & Stanke, 2019; Zdobnov et al., 2021). These gene models were annotated using the software eggNOG-mapper version 2 eggNOG version 5.0 database (Cantalapiedra et al., 2021; Huerta-Cepas et al., 2019). Genomic assembly and gene model predictions were evaluated for completeness using BUSCO version 5.5.0 in both genome and protein modes, compared to a set of conserved chlorophyte genes provided in OrthoDB (Kuznetsov et al., 2023; Seppey et al., 2019).

Data Access

Raw sequencing data and whole genomic assembly for this project is available at the National Center for Biotechnology Information through BioProject PRJNA1151728. Assembled contigs, gene models, and annotations for the *C. pacifica* genome are available on figshare (10.6084/m9.figshare.26824903). All supplemental materials are also included in the figshare link.

Phylogenetic Analysis

For constructing the phylogenetic tree, we considered all species under the Chlorophyta taxon whose gene annotations were made available on the NCBI genome platform (https://www.ncbi.nlm.nih.gov/datasets/genome). We incorporated 1,519 genes from the Chlorophyta odb10 dataset, as identified by the Benchmarking Universal Single-Copy Orthologs (BUSCO) initiative (Manni et al., 2021). For each BUCSO gene, we identified its orthologue in each species by employing the protein mode of BLAST and selected the gene with the lowest e-value (Johnson et al., 2008). Subsequently, we performed multiple-sequence alignment using MUSCLE and generated the corresponding gene trees using CLUSTALW2 (Edgar, 2004; Larkin et al., 2007). Finally, the species tree was estimated from the gene trees using ASTRAL-III (C. Zhang et al., 2018).

Metabolic Pathway

The ALGAEpath tool was used to extract the β-Alanine metabolic pathway information for *Chlamydomonas reinhardtii* (Zheng et al., 2014). To identify orthologous genes in *Chlamydomonas pacifica*, NCBIblastp performed a gene blast search against the *C. reinhardtii* genes involved in this pathway. To find the corresponding orthologs in *Chlamydomonas pacifica*, local NCBI BLASTP searches were conducted employing the Biopython package (version 1.81) in Python, with the cutoff e-value set at 0.001 (Altschul et al., 1990). Subsequently, the discovered orthologs underwent functional validation through the EggNOG tool (Huerta-Cepas et al., 2019).

Metabolomics and Lipidomics

Supernatant and pellet samples from algal cultures were prepared through lyophilization and resuspended with ribitol as an internal standard for consistent quantification. Following the adapted protocol from Hollin et al. (2022), a biphasic extraction using a methyl tert-butyl ether and methanol solution facilitated the separation of metabolites, which were then analyzed for lipidomics at the UC Riverside Metabolomics Core Facility using a G2-XS quadrupole time-of-flight mass spectrometer and for polar metabolites using a Thermo 1300 GC coupled to an ISQ7000 mass spectrometer (Hollin et al., 2022). Data analysis incorporated advanced software like Progenesis Qi and MS-DIAL for peak identification, normalization, and annotation, employing various databases and proprietary tools for comprehensive metabolite profiling. Detailed methodological procedure is available at Supplementary Material (see **Supplementary Method** section).

Strain profile

Carbon and Nitrogen Assimilation

To evaluate carbon and nitrogen assimilation, HSM and HSM without nitrogen agar plates were prepared using Thermo Fisher Scientific's Thermo Scientific™ Nunc™ OmniTray™ Single-Well Plate (Catalog number: 242811). The composition of the media is outlined in the Supplementary Material (**Supplementary Table 1a-d**). Each plate, containing approximately 35 ml of 1.5% agar medium, was prepared. Subsequently, 1 ml of algae culture was evenly spread across the surface of the plate. Once the cells had dried, to the corners of the plate, 500 ul of a 1% agarose solution containing HSM with varying nitrogen sources or different carbon source solution was gently dispensed onto the surface creating a small mound above the agar medium. The carbon source plates were left on the lab bench in low light approximately 8 µmol photons m^2 s^{-1} and nitrogen source plates were grown photosynthetically in 80 µmol photons/m^2s^1 of light.

pH Tolerance

To compare the strain's capacity to grow in different pH and salinity, Nunc® OmniTray (Merck KGaA, Darmstadt, Germany) were prepared with agar HSM. The pH gradient was created by adding and spreading 60 µL of 3.3M H_3PO_4 on one side of the plate, followed by adding 60 µL of 10M KOH on the opposite side. The plates were left to equilibrate for 2 days, so the pH gradient was formed and samples were spread across the pH gradient in parallel sections of the plate for pH tolerance capacity (**Supplementary Figure 1**).

Salt Tolerance

To compare the strain's capacity to grow in different salinity, Nunc® OmniTray (Merck KGaA, Darmstadt, Germany) were prepared with agar HSM media with 150mM NaCl. The salt gradient was created by removing a section of 1.5 cm in one of the sides of the plate, and adding a melted 1.5% agarose solution of 5M NaCl. To further compare the strain's capacity to grow in different salinities, growth curves were prepared in HSM with varying additional concentrations of NaCl, grown in 96 well plates, shaken at 800 rpm with continuous light at 80 µmol photons m^2 s^{-1} from white neutral LEDs. Growth was monitored by optical density measured

Temperature Tolerance

To compare the strains' capacity to temperature, cells were grown in HSM acetate until stationary phase and exposed to different temperature values, ranging from 37.5°C to 44.5°C. The cells were exposed for 24 hours and plated on an agar HSM plate to recover surviving cells. Briefly, 150 µL of culture was added to 96 well PCR plates, 5 µL samples were taken to an HSM acetate plate and placed to grow to be used as an initial culture condition. The rest of the samples were sealed with a PCR plate seal. The plates were incubated in a 96-well T100 thermal cycler (Biorad, Hercules, CA, USA) using fixed temperature gradients for each row. After 24 hours of incubation, the cells

were resuspended by pipetting, and a 5 µL sample was added in a HSM acetate plate. After culture spots were dried, the plates were placed on growing conditions. After 5-7 days, images were taken from each plate.

Light Tolerance

To assess the light tolerance of different strains, cultures were grown to stationary phase in either HSM acetate or TAP media. Subsequently, 200 µL of each culture was uniformly spread along the length of an OmniTray™ Single-Well Plate (Catalog number: 242811) containing HSM agar. *Chlamydomonas reinhardtii*, known for its sensitivity to high light, served as a control and was tested in parallel to the test strains (Erickson et al., 2015; Virtanen et al., 2021). The plates were then positioned 9 cm away from a 1000W Mastiff GrowL® LED grow light, utilizing both blue and red LEDs to simulate high light conditions. To create a gradient of light exposure, plates were aligned so that portions were directly beneath the LEDs while others extended beyond the light's direct reach. Protective shading was placed in one of the corners of each plate, to ensure survival of some cells as initial inoculum control. The photosynthetic photon flux density (PPFD) was measured across the plate surface at 5 mm intervals, repeated three times. The resulting data, excluding the initial shadowed area and the intense central light zone of the panel, depicted a linear PPFD gradient, as detailed in **Supplementary Figure 2**.

Phototaxis

To investigate phototaxis in *Chlamydomonas pacifica* 402, cells were cultured on HSM agar plates for 5-7 days. Subsequently, the mature cells were harvested and resuspended in nitrogen-free HSM media to trigger gametogenesis and enhance flagellar movement. The prepared cells were then distributed into a 6-well plate and positioned before a light source, allowing them to exhibit phototactic behavior for 10 minutes. Photographic documentation was performed using a Canon EOS camera, capturing images at the start (t=0 min) and after 10 minutes of light exposure. To visualize the cells, photographs were taken against both a white backdrop to highlight their green pigmentation and a blue backdrop with an orange filter to accentuate chlorophyll fluorescence, providing a view of the cells' phototactic response.

Motility

To measure cell movement speeds, we followed the method described in Molino et al., (2022), with a few modifications. Cells were grown in HSM acetate agar plates for 5 days, scraped, and resuspended in HSM media without the nitrogen source. The cells were kept in the dark until testing. The slides were prepared using glass slides with Frame-Seal™ Slide Chambers, 15 × 15 mm, 65 µL and sealed with a cover slip. The cells were observed with a Nikon microscope equipped with a Nikon DS-Qi2 camera, and the recorded video was analyzed with ImageJ's plugin TrackMate (6.01) (Tinevez et al., 2017). A more detailed protocol can be found in dx.doi.org/10.17504/protocols.io.bsw5nfg6. R version 3.6.3 (2020-02-29) running in the RStudio v1.2.5042 IDE was used to import and process data and generate the plots as a density plot.

Assembly of transformation vectors

All restriction enzymes utilized in this study were sourced from New England Biolabs (Ipswich, MA, USA). These constructs were developed using the pBlueScript II + KS (pBSII) backbone. The vector pAH04mCherry was previously described by Molino et al., (2018), and it contains genetic elements from *C. reinhardtii*. The vector pJPSHxPHL7 was assembled using genetic elements from the assembled genome from *C. pacifica* 402. We identified the β-Tubulin A 2 gene and its structures. The vector was then assembled using the promoter, introns one and two, and the 3'UTR region of the gene. We added the hygromycin resistance marker codon optimized to *C. reinhardtii* followed by the foot-and-mouth-disease-virus 2A self-cleavage peptide (FMDV-2A), the SP7 signal peptide and the codon optimized sequence for PHL7 (**Supplementary Figure 3a**) (Sonnendecker et al., 2021). The sequence and the complete map can be observed in **Supplementary Figure 3b**.

Transformation

Transformation of *C. pacifica* was conducted using electroporation, following the protocol outlined at Molino et al., (Molino et al., 2022). In summary, cells were cultured to reach mid-logarithmic growth phase (3–6×10^6 cells/mL) in HSM acetate medium, maintained at 25 °C with constant light exposure (80 µmol photons/m^2s) and shaking at 150 rpm. The cells were then concentrated by centrifugation at 3000 g for 10 minutes and resuspended to a density of 3–6×10^8 cells/mL using the MAX Efficiency™ Transformation Reagent for Algae (Catalog No. A24229, Thermo Fisher Scientific). For the electroporation, a mixture of 250 µL of this cell suspension and 1000 ng of a vector plasmid digested with XbaI and KpnI enzymes was chilled on ice for 5–10 minutes within a 4-mm width cuvette compatible with the Gene Pulser®/MicroPulser™ system (BioRad, Hercules, CA). The cell-DNA mixture was then electroporated using the GenePulser XCell™ device (BioRad, Hercules, CA), applying a pulse of 2000 V/cm for 20 microseconds. Following electroporation, the cells were transferred into 10 mL of HSM acetate medium and incubated under gentle agitation (50 rpm) in ambient light conditions (around 8 µmol photons/m^2s) for an 18-hour recovery period. Post-recovery, the cells were again concentrated by centrifugation, resuspended in 600 µL of HSM acetate medium, and evenly spread onto two HSM acetate agar plates, each containing different antibiotics according to the vectors used. The zeocin (Zeo) concentration was 10 µg/mL and hygromycin (Hyg) was 30 µg/mL. The plates were then incubated under a light intensity of 80 µmol photons/m^2s at 25 °C until visible colonies developed.

The pJPSHx1PHL7-transformed cells were plated onto TAP agar plates containing 0.75% (v/v) Impranil® DLN, a colloidal polyester-PUR dispersion, and 30 µg/mL hygromycin (Liu et al., 2021) . These selective media plates were prepared by making 1 L of TAP media with agar and autoclaving to sterilize. Once the media has cooled to 55°C, hygromycin was added to a final concentration of 30 µg/mL and 7.5 mL of Impranil® DLN was added to achieve 0.75% (v/v). After thoroughly mixing, the media was poured into Petri dishes and allowed to solidify.

Mating

The mating assays were performed in line with the methodology outlined by (Findinier, 2023). Initially, recombinant *Chlamydomonas pacifica* strains CC-5697 harboring the pJPSHx1PHL7 (Hyg) vector and CC-5699 harboring the pAH04mCherry vector (Zeo) were cultured on HSM acetate agar plates for 7 days. Post-cultivation, the cells were harvested using a sterile loop, resuspended in nitrogen-depleted HSM media, and subjected to light exposure (80 µmol photons/m^2s) overnight without agitation. Each strain possessed a distinct antibiotic resistance marker, with one strain being resistant to zeocin and the other to hygromycin. Following light exposure, the strains were combined and incubated in darkness for at least 24 hours without disturbance. After this dark incubation phase, the cells were centrifuged down at 2000g for 5 min, resuspended in fresh media, and placed under standard growth conditions to facilitate the emergence of daughter cells. After 2-3 days, these cells were then plated on selective media containing both antibiotics, enabling the identification and selection of progeny cells that inherited resistance markers from both parent strains.

Data analysis

R version 3.6.3 (2020-02-29) running in the RStudio v1.2.5042 IDE was used to import and process data, generate the statistical summary, and generate the plots for motility. The growth curve was performed using Microsoft Excel 365 (Version 16.0, Microsoft Corporation, Redmond, WA, USA).

Results

Genome features

This study presents the first comprehensive multi-omics characterization of a newly discovered extremophile green alga, *C. pacifica*. This investigation employed a multifaceted approach, delving into the full suite of traits distinguishing *C. pacifica* from the well-studied model *Chlamydomonas reinhardtii.* Alongside this detailed phenotypic comparison, omics analyses were employed to illuminate this organism's underlying genomic, transcriptomic, and metabolic context. Later, we also showed high pH tolerance in *C. pacifica* that might raise interest in this cell line to unlock biotechnological applications.

C. pacifica exhibits a genome size (121 Mbp) and lower GC content (61%) compared to *C. reinhardtii* and it harbors 17,829 protein-coding genes, comparable to its well-studied counterpart (i.e. 16,795 genes in CC-503 v6.1 *C. reinhardtii*) (Craig et al., 2022). Furthermore, to assess the completeness of the annotated *C. pacifica* genome, Benchmarking Universal Single-Copy Orthologs (BUSCO), a tool that evaluates the presence of a highly conserved

set of single-copy genes in most Chlorophyta lineages, was employed. The BUSCO analysis revealed 91.3% completeness, indicating minimal gene loss and the comprehensiveness of the genome annotation. Analysis of both strains revealed a correlation in codon usage patterns (**Supplementary Figure 4**). The similar codon usage patterns in *C. reinhardtii* and *C. pacifica* imply that DNA sequences optimized for *C. reinhardtii* are likely well-translated in *C. pacifica*, thus reducing the need for extensive codon optimization for genetic engineering applications when starting from the more available *C. reinhardtii* vectors.

The study also assessed the occurrence of genes involved in mating processes, revealing homologies between *C. reinhardtii* and *C. pacifica* in several mating-related genes (**Supplementary Table 2**) (Ferris et al., 2002). These include genes unique to MT- gametes (mtd1, mid), a MID-dependent activation protein (GSM1), the sexual agglutination gene (SAG1), sexual adhesion gene (SAD1), the HAP2 gene responsible for membrane pore formation during mating, the nuclear fusion protein GEX1, the gametogenesis-active matrix metalloprotease gene Mmp1, the mating type plus-specific protein GSP1 active in zygotes, and the gamete fusion protein Fus1 (Kubo et al., 2001; Lin & Goodenough, 2007; Ning et al., 2013; Pinello & Clark, 2022). The sequence similarity among these genes varied significantly, with identity ranging from 4.6% to 37.1%, indicating diverse evolutionary rates (**Supplementary Table 2**). We constructed a phylogenetic tree including 42 green algae strains positioned *C. pacifica* within the core-Reinhardtinia clade, closely related to *Chlamydomonas sp.* 3222 (**Figure 1**) (Nelson et al., 2019). This finding sheds light on the evolutionary relationships between *C. pacifica* and other green algae species, providing valuable insights into its ancestry and potentially shared adaptations. The closest available strain to *C. pacifica* is *Chlamydomonas sp. 3222* (available at Chlamydomonas Collection, with index CC-5164), whose similarity with *C. pacifica* will be discussed further below (Nelson et al., 2019).

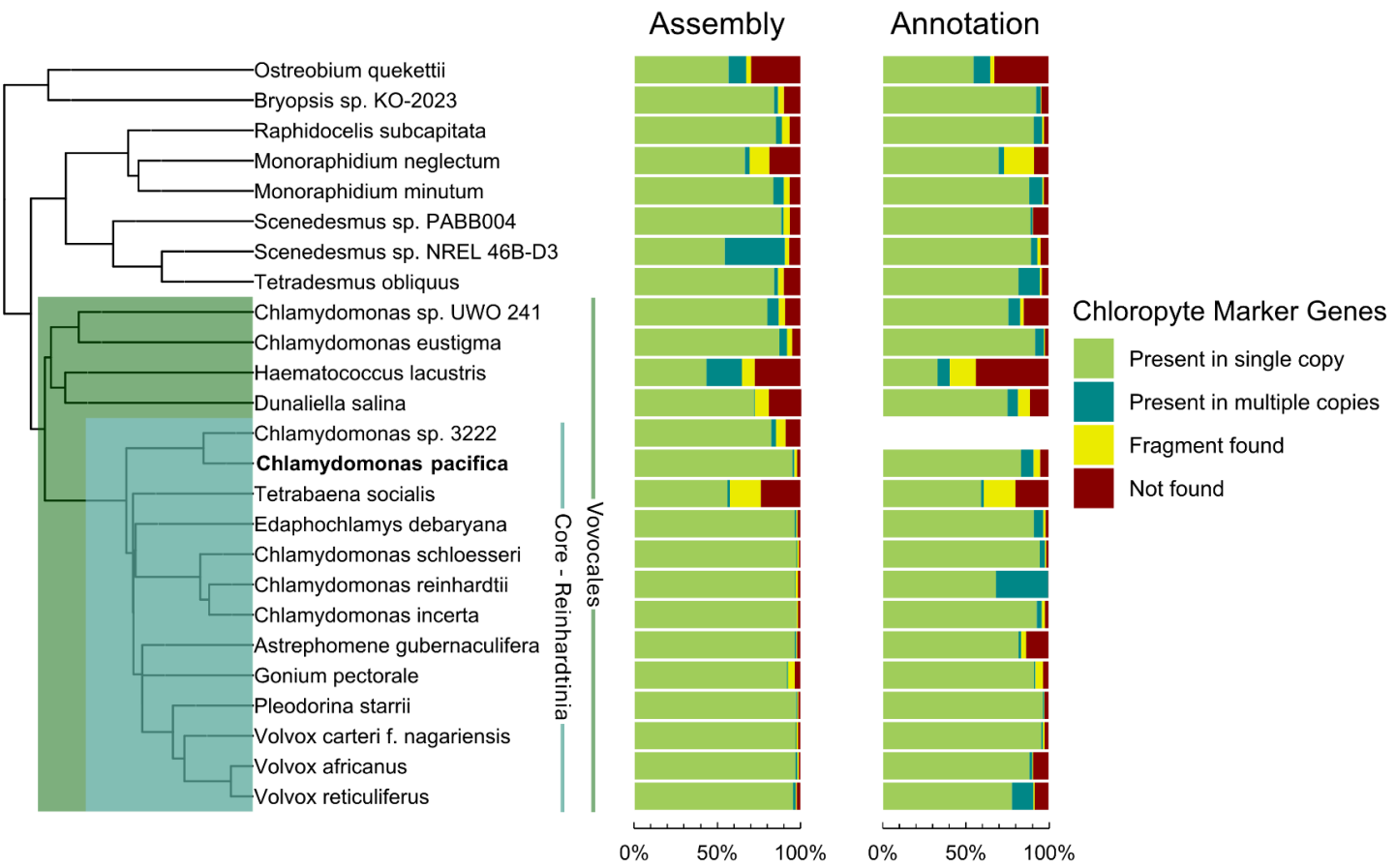

Figure 1: Phylogenetic distribution of assembled chlorophyte genomes based on average amino acid identity. Completeness bar graphs adjacent to the phylogenetic tree display BUSCO scores for the genome assembly and gene models, if publicly available. *C. pacifica* completeness of assembled and annotated chlorophyte genomes is consistent with other members of the Vovocales (Seppey et al., 2019).

Cell Profiling

In this study, a detailed characterization of four Chlamydomonas strains were conducted with a focus on their nutrient assimilation capabilities and environmental resilience. The phylogenetic analysis (presented in the preceding section) revealed that *C. sp.* 3222 is closely related to the newly identified *C. pacifica* strains 402 and 403. Alongside the comparison with the well-established *C. reinhardtii*, we evaluated their carbon and nitrogen uptake efficiencies. Their tolerance to a range of pH levels, salinity, temperatures, and light conditions were tested. This comprehensive assessment aims to delineate the physiological and ecological niches of these strains, with a particular focus on understanding the similarities and differences between the closely related *C. sp. 3222* and *C. pacifica* strains, thereby shedding light on their potential for adaptive strategies and applications in biotechnological settings.

Cell Morphology

Microscopy pictures of *C. pacifica* strains 402 and 403 were captured through differential interference contrast (DIC) microscopy and fluorescence microscopy techniques (**Figure 2**). The DIC images revealed the structural details of the cells, including the presence of two flagella per cell, each with an approximate length of 10 µm. This morphological feature is essential for the cells' navigation and positioning in their environment, which is crucial for light capture, avoiding unfavorable conditions, and mating.

The fluorescence microscopy images highlighted the chloroplasts, revealing the distinct thylakoid structures (**Figure 2**). A darker region within the chloroplasts was also observed, which is likely indicative of a pyrenoid—an organelle linked to carbon fixation. Furthermore, we identified a gene in *C. pacifica* (anno1.g15702.t1) that shows the closest similarity to the *C. reinhardtii* Essential Pyrenoid Component 1 (EPYC1, also known as LCI5) gene, with 52.49% identity (99% coverage and an e-value of 1e-29). EPYC1 is known to associate with Rubisco holoenzymes to form the pyrenoid matrix (Mackinder et al., 2016). These findings suggest that pyrenoids, a common feature in *C. reinhardtii*, may be present in strains 402 and 403 of *C. pacifica*, potentially sharing a similar carbon fixation mechanism as this well-studied species (Mackinder et al., 2016).

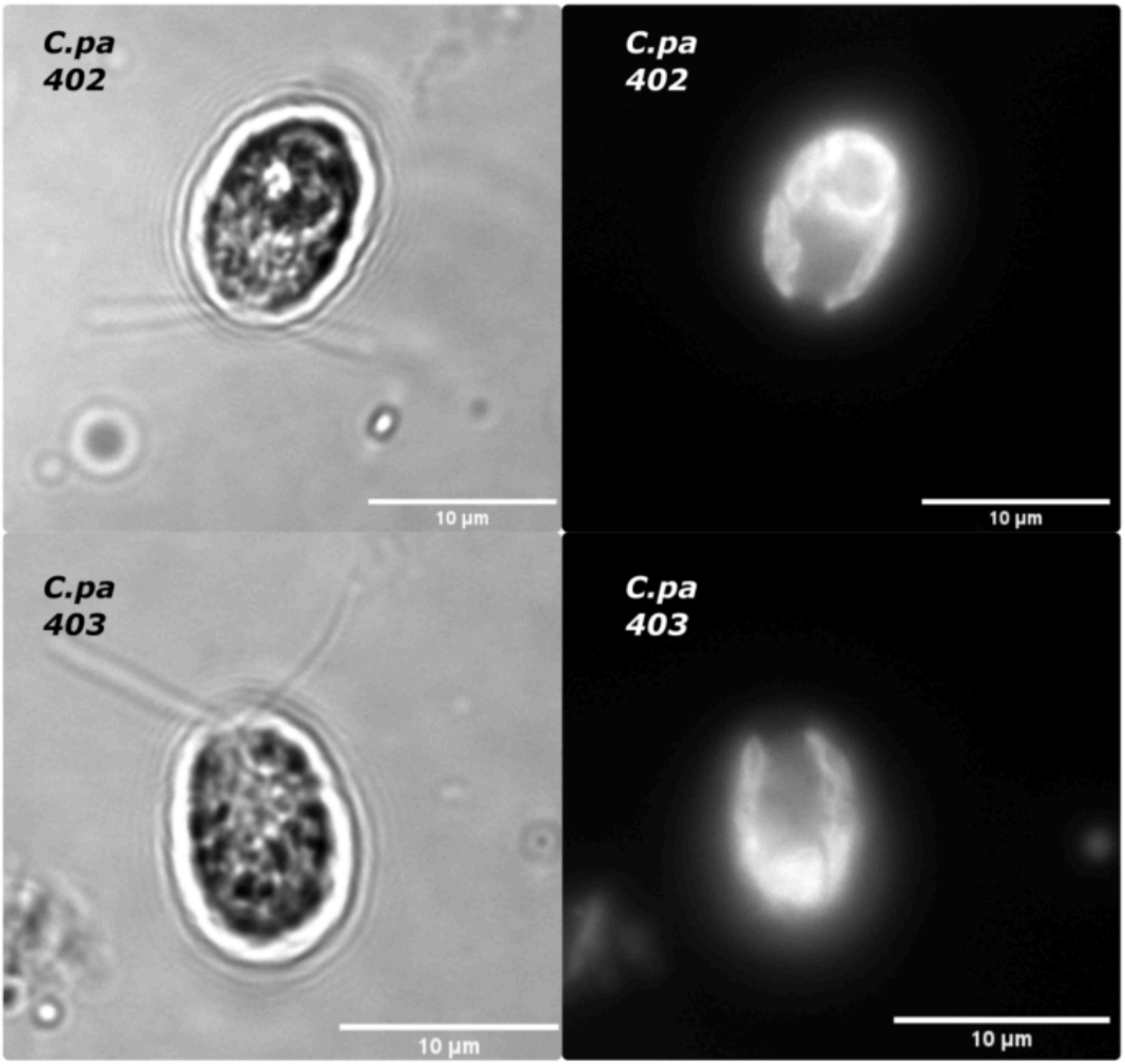

Figure 2: Microscopic analysis of *Chlamydomonas pacifica* strains 402 and 403. The left images display cells of *C. pacifica* strains 402 (top) and 403 (bottom) visualized using Differential Interference Contrast (DIC) microscopy, which reveals detailed cellular structures. The right images correspond to the same cells, highlighting the chlorophyll autofluorescence, indicative of the chloroplasts within the cells. The scale bars represent a length of 10 µm.

Phototaxis

To observe the cell's phototaxis capacity we placed *C. pacifica* in HSM without nitrogen and exposed to light from one side of the well. The starving conditions is a stimulus to flagella activity, and the cell when exposed to light can use the light cue to swim in its direction (**Figure 3**). We capture two sets of images: the initial moment (t=0 min) and after 10 minutes (t=10 min), labeled "White" and "Chloro", indicating the white backlight used and indicating that we used chlorophyll fluorescence to observe cells' position in the photograph. At the initial time, the cells are evenly distributed across the wells. After 10 minutes, there is a clear migration of the cells away the light source, congregating at the right corner of the wells, particularly noticeable in the "Chloro" condition. Lower light was present in the right corner. This movement indicates a negative phototactic response of the algae cells, moving away the light to a more optimal intensity to perform photosynthesis or for other biological processes necessitated by light.

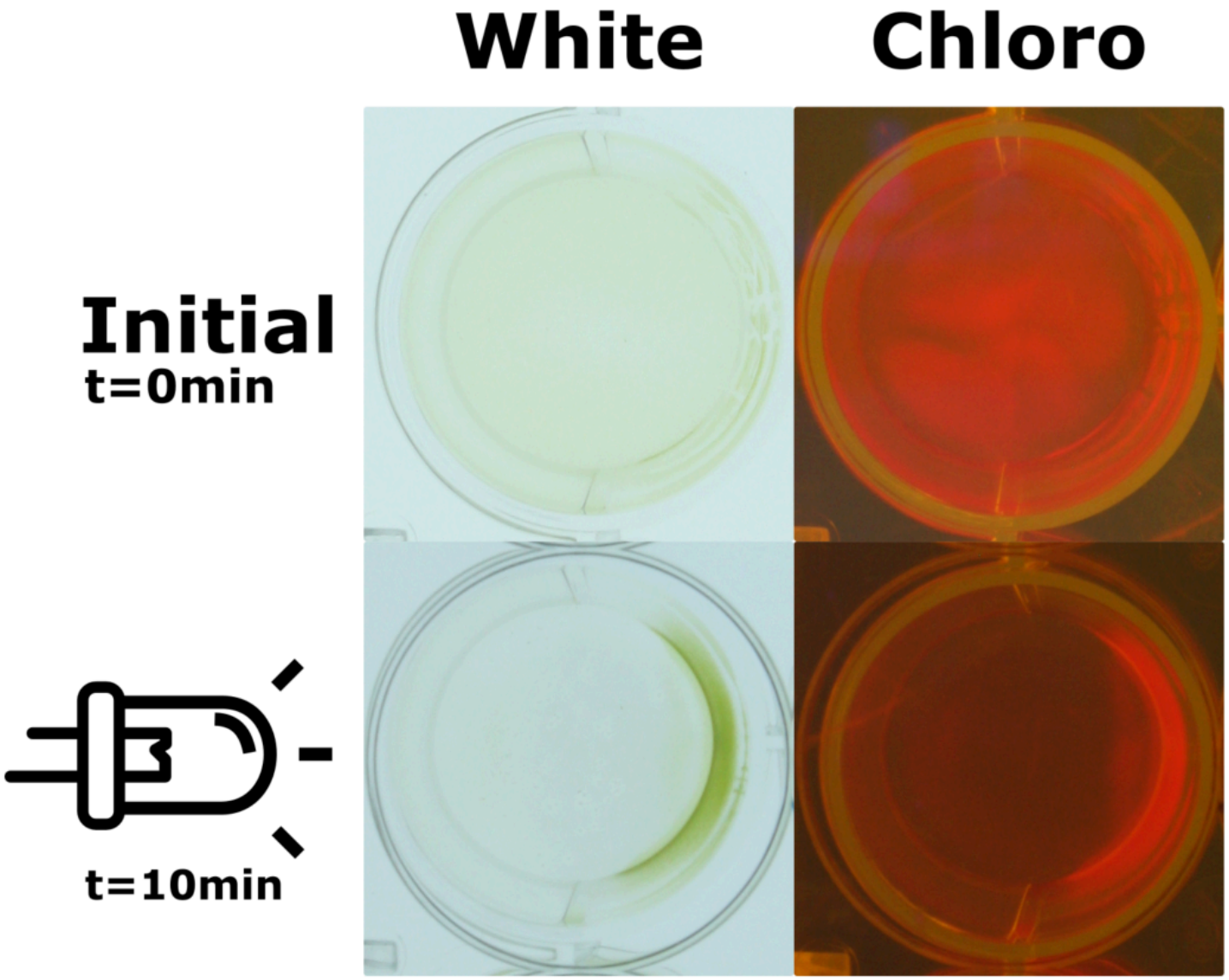

Figure 3: Phototaxis experiment demonstrating *C. pacifica* motility and response to light. The top panel shows strain 402 at the initial moment without light stimuli. The bottom panel shows the phototaxis behavior of the cell after 10 min of exposure to light in the left side of the well, Cells were kept in HSM-N media, with a light intensity of 300 uE/m^2s. Photos were obtained with a white transilluminator (left panel), and a blue transilluminator with an orange light filter (right panel) to observe Chlorophyll pigment fluorescence.

Carbon and Nitrogen Assimilation

In our investigation, we examined the growth dynamics of two novel Chlamydomonas species, *C. pacifica* strains 402 and 403, in comparison with the well-studied *C. reinhardtii* and *C. sp. strain 3222*, under distinct illumination regimes tailored to probe their photosynthetic and non-photosynthetic metabolic capacities. Nitrogen-source plates, incubated under continuous light (80 µmol photons.m^{-2}.s^{-1}), facilitated a predominantly photosynthetic growth mode (**Figure 4**). In contrast, carbon-source plates were exposed to low light (approximately 8 µmol photons m^2 s^{-1}) to mitigate but not abolish photosynthetic activity, thereby accentuating heterotrophic growth potential (**Figure 5**).

Under continuous illumination, all strains demonstrated the capacity to assimilate the provided nitrogen sources, consistent with established research indicating efficient integration of such sources by Chlamydomonas species (Fernández et al., 2009). Notably, the novel *C. pacifica* strains exhibited a distinctive growth response to urea and sodium nitrate, as *C. reinhardtii* (**Figure 4**). This versatility in nitrogen source bears significance for large-scale algal culture systems, where the choice of nitrogen source can profoundly impact both sustainability and economic viability of biotechnological processes.

Conversely, the carbon-source assessment revealed that in the vicinity of the acetate, a noticeably darker green pigmentation was observed for *C. pacifica* strains, indicative of enhanced growth surpassing that attributable solely to photosynthesis (**Figure 5**). This is particularly significant given the low-light conditions, which suggests a capacity for acetate assimilation in these strains, potentially via acetate activation and subsequent entry into the Tricarboxylic Acid Cycle (TCA) cycle, a metabolic pathway that has been previously described in microalgae (Bogaert et al., 2019). On the other hand, the lack of such pigmentation near other carbon sources (sucrose, glycerol, and glucose) implies ineffective assimilation under the given conditions, with growth primarily reliant on photosynthesis, as evidenced by similar coloration to the plate center. The *C. pacifica* strains demonstrated an ability to utilize acetate for growth under low-light conditions, an attribute relevant for bioreactor systems where light is limited.

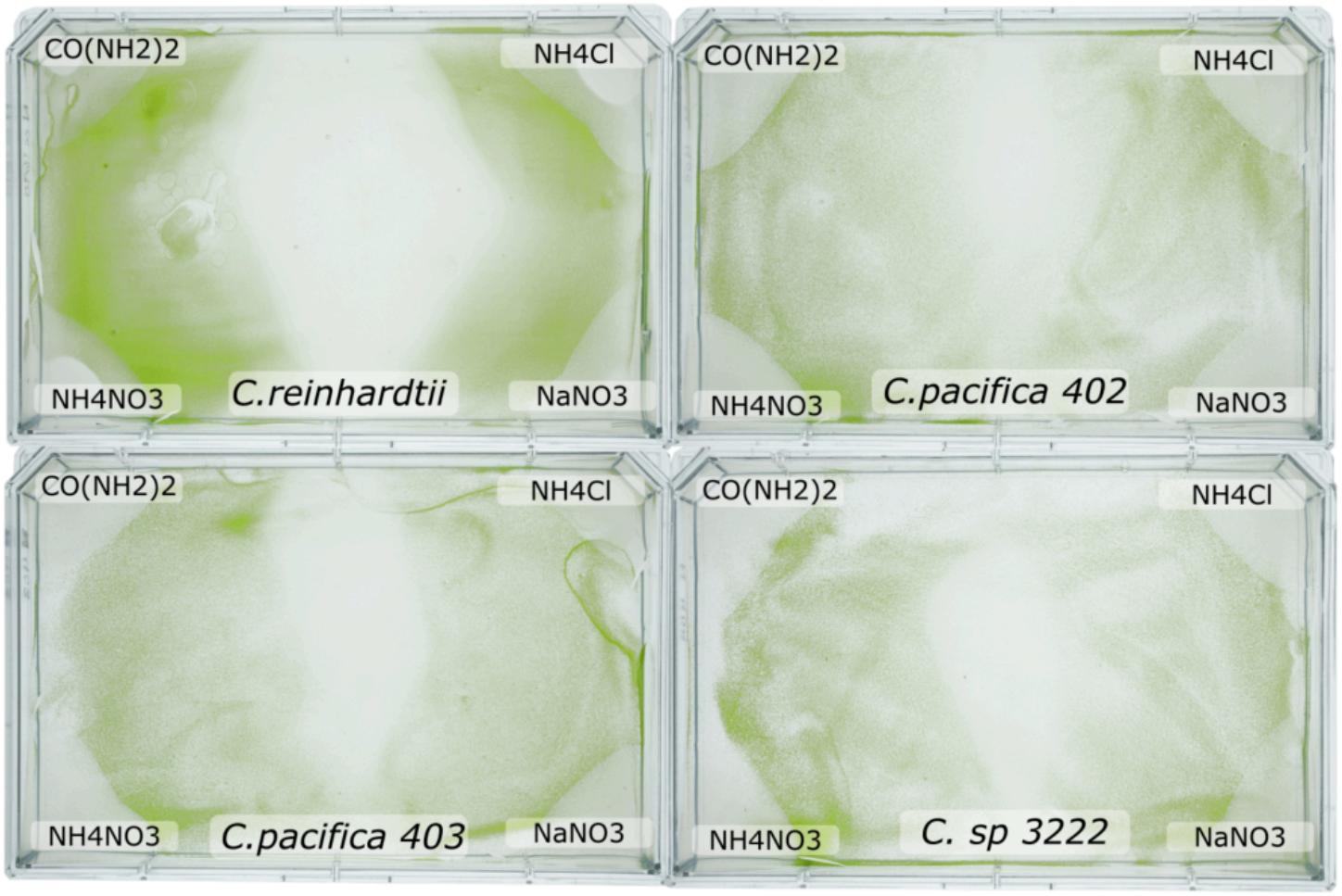

Figure 4. Comparative Growth Responses of *Chlamydomonas* Species to Different Nitrogen Sources. Petri dishes exhibit the growth of three *Chlamydomonas* strains: *C. reinhardtii*, *C. pacifica* strains 402 and 403, and *C. sp.* strain 3222, cultured in HSM without nitrogen media. The corners were supplemented with varying nitrogen compounds at 9.34 mM of nitrogen atoms. From left to right, the nitrogen sources provided are urea (CO(NH2)2), ammonium chloride (NH4Cl), sodium nitrate (NaNO3), and ammonium nitrate (NH4NO3). The center portion serves as a negative control.

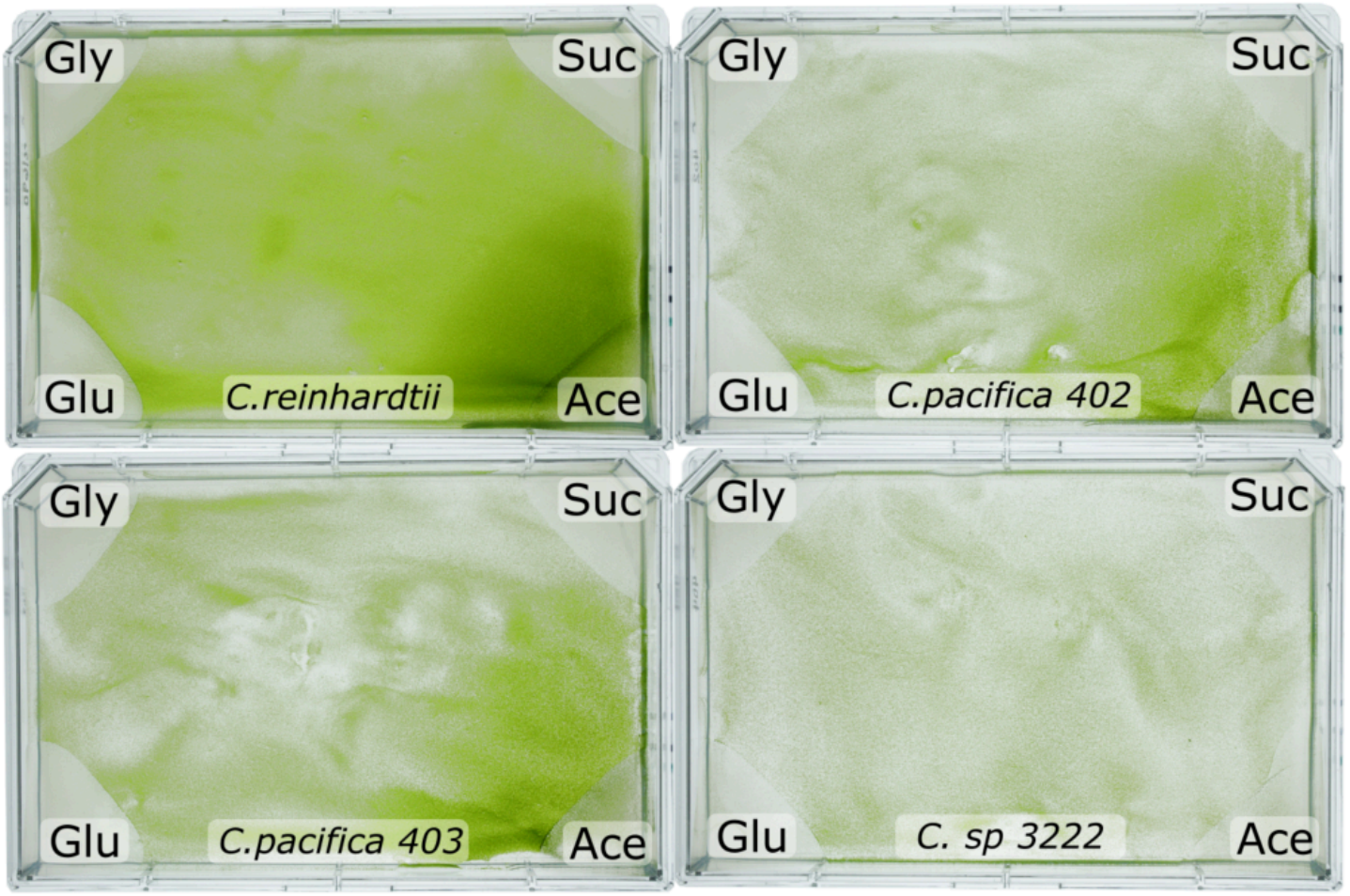

Figure 5. Differential Growth of *Chlamydomonas* Strains on Various Carbon Sources. The petri dishes demonstrate the growth patterns of *C. reinhardtii*, *C. pacifica* strains 402 and 403, and *C. sp.* strain 3222, when cultured on HSM media supplemented with distinct carbon sources. The carbon compounds tested include acetate (Ace), sucrose (Suc), glycerol (Gly), and glucose (Glu), arranged clockwise from the top left corner of each dish. The variation in green pigmentation intensity across the media indicates the efficiency of carbon utilization by each algal strain. Plates were incubated at room light to reduce photosynthetic growth.

pH Profile

The pH tolerance of *Chlamydomonas* strains was assessed through a gradient plate assay (**Figure 6**), revealing significant variations in the capacity of these strains to thrive across different pH levels. The mesophilic nature of *C. reinhardtii*, was observed with an optimal growth within a moderate pH range, aligning with previous characterizations of its preferred neutral environments (Dhaliwal et al., 2017). This species' adherence to mesophilic growth conditions highlights its evolutionary tuning to stable pH environments, a trait that could have implications for its ecological distribution and suitability for controlled bioprocesses. In contrast, the *C. pacifica* strains 402 and 403, alongside *C. sp.* strain 3222, exhibited a more extensive pH tolerance, thriving in conditions

extending from pH 6 to greater than pH 10. The broader pH adaptability of these strains, especially when considered in conjunction with their phylogenetic proximity, underscores a potentially shared evolutionary capacity for environmental resilience that could be leveraged in open ponds cultures in which the elevated pH can protect the culture from pests.

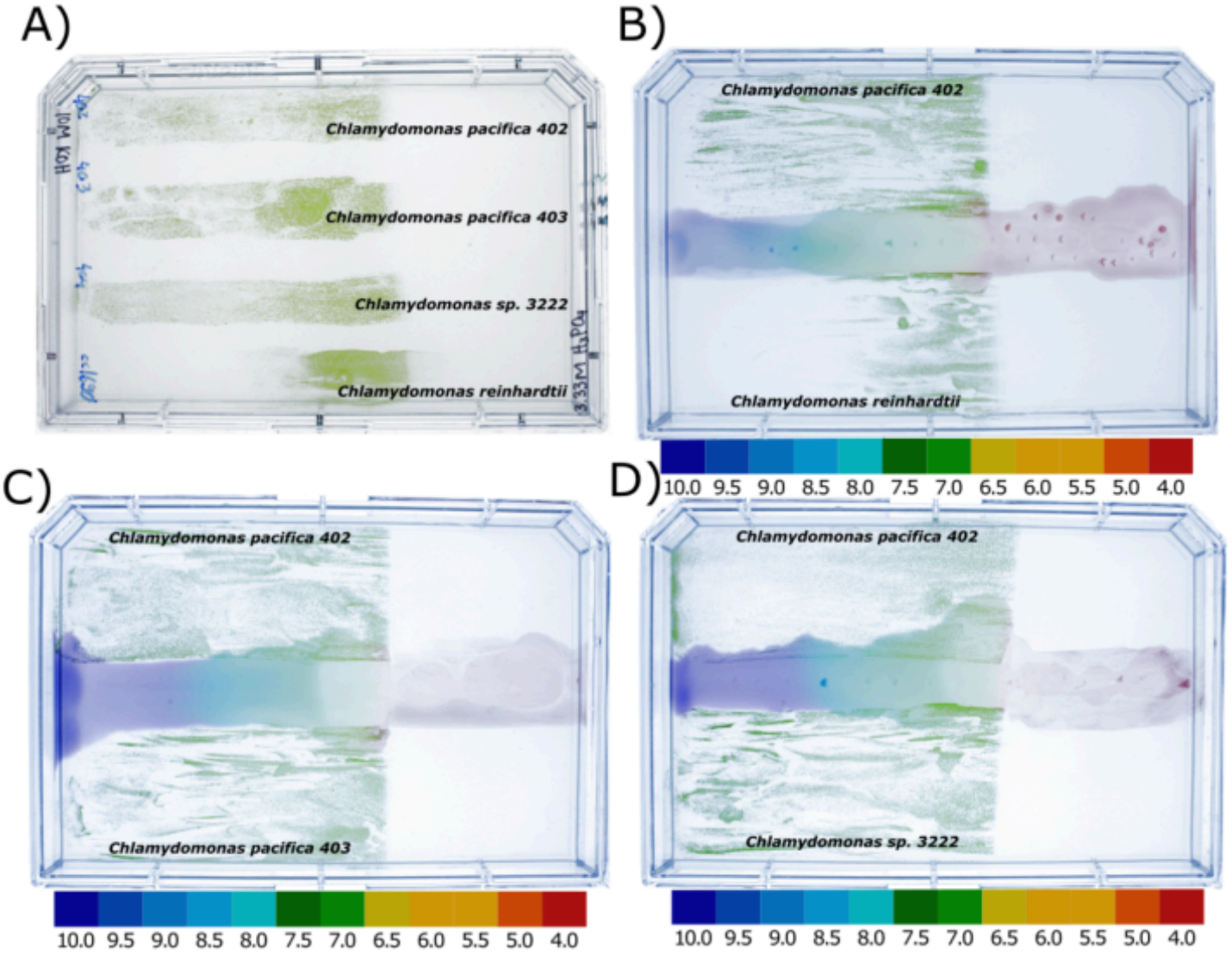

Figure 6: pH Gradient-Based Growth Profiling of *Chlamydomonas* Strains. The growth patterns of *C. reinhardtii*, *C. pacifica* strains 402 and 403, and *Chlamydomonas sp*. strain 3222 are demonstrated across a pH gradient. **A**) Growth of *C. pacifica* strains 402 and 403, *C. sp.* strain 3222, and *C. reinhardtii* across a pH gradient. **B**) Growth response of *C. pacifica* strain 402 and *C. reinhardtii* to the pH gradient. **C**) Growth of *C. pacifica* strains 402 and 403 across a pH gradient. **D**) Growth of *C. pacifica* strain 402 with C. sp. strain 3222 across a pH gradient. The gradient was established by the application of 60 µL of 3.3M H3PO4 to the right side and 120 µL of 10 M KOH to the left side of each agar plate. A universal pH indicator (Fisher Chemical™ Universal pH Indicator System) was used to visualize the pH levels, with color changes indicating variations in pH across the plate. The differential growth observed reflects the varying capacities of the strains to tolerate and

thrive under different pH conditions, providing insights into their adaptability and potential for cultivation in diverse environmental settings.

Salt Profile

To investigate the ability of the *Chlamydomonas* strains to withstand osmotic stress, we cultured them in HSM amended with varying concentrations of NaCl, which served to mimic different osmotic pressures found in water ecosystems (**Figure 7**). The strains *C. pacifica* 402 and 403 were found to sustain growth at salinity levels elevated by an additional 300 mM NaCl, with strain 403 showing slightly better growth efficiency under these conditions. This osmotolerance was further explored through NaCl gradient plates, where strains 402, 403, and *C. sp.* strain 3222 exhibited comparable and notably higher salt tolerances than *C. reinhardtii,* which displayed growth within a more limited saline range. The gradient plate results indicated that the three strains, including *C. sp.* strain 3222, possess similar capacities to tolerate brackish salinity levels. These findings point to a significant osmoregulatory ability in strains 402 and 403, as well as *C. sp.* strain 3222, highlighting their potential application in biotechnological processes that require robustness to saline conditions, such as those found in coastal or estuarine aquaculture systems.

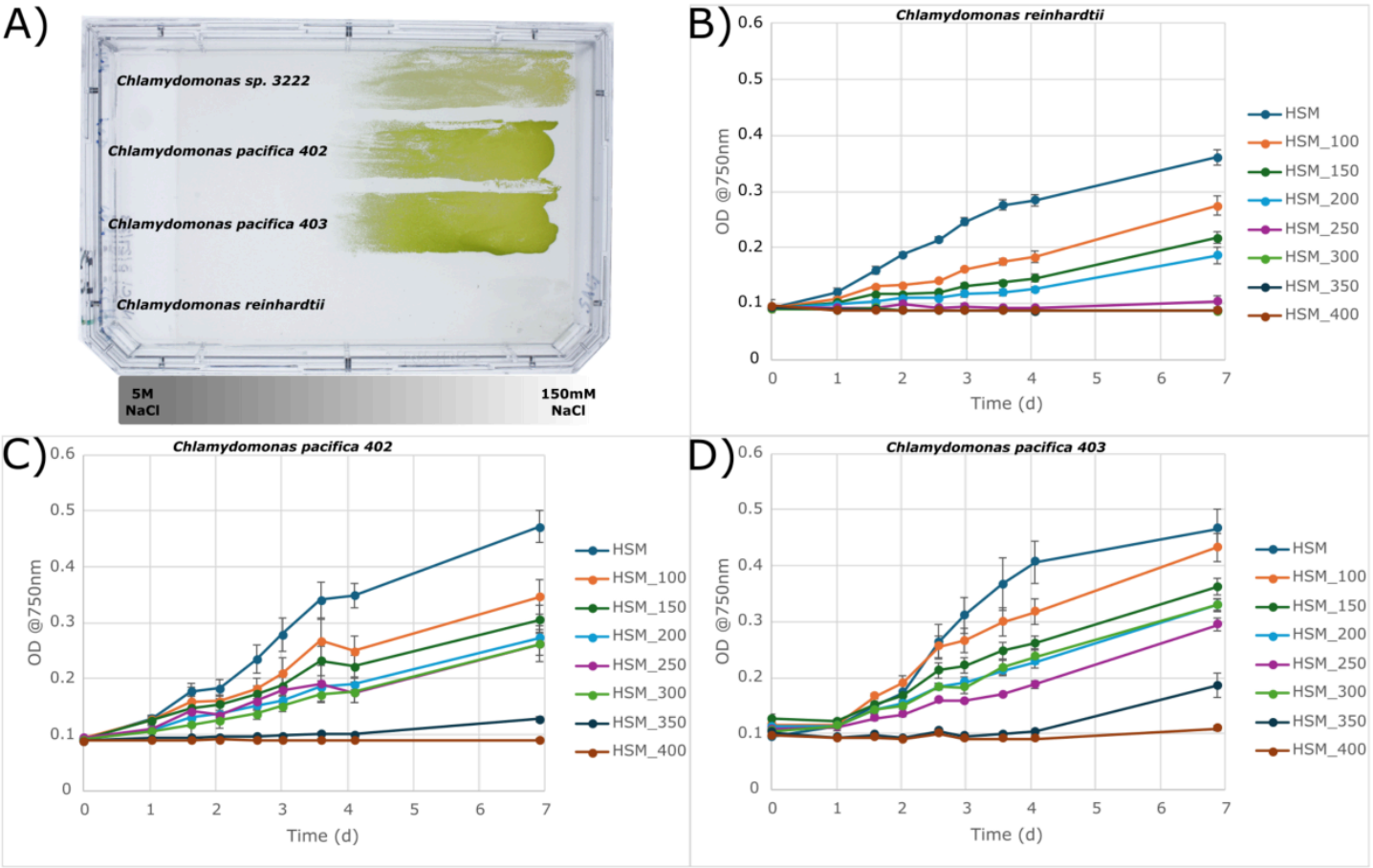

Figure 7: Salinity Tolerance of Chlamydomonas Strains. A) NaCl gradient plate delineating the comparative growth of *C. reinhardtii*, *C. pacifica* strains 402 and 403, and *C. sp.* strain 3222, with the left part containing high

salinity (5 M NaCl) and the right side moderate salinity (150 mM NaCl). **B-D**) Growth curves over a seven-day period for *C. reinhardtii* (**B**), *C. pacifica* 402 (**C**), and *C. pacifica* 403 (**D**) in high salt media (HSM) with incremental NaCl additions ranging from 0 to an additional 400 mM. The data illustrate the relative growth in optical density (OD) at 750 nm.

Temperature Profile

The thermal tolerance assay conducted on the Chlamydomonas strains provides critical insights into their potential for cultivation in global regions with high-temperature variability, especially semi-arid areas where competition with agriculture is minimal. In these regions, temperatures can frequently exceed 40°C (Winckelmann et al., 2015), necessitating robust thermotolerant strains for successful algal cultivation. *C. pacifica* strains 402 and 403 and *C. sp*. strain 3222 exhibited considerable resilience to elevated temperatures, withstanding up to 41.9°C (**Figure 8**). This degree of thermotolerance surpasses that of *C. reinhardtii* CC1690, which preferred cooler conditions, typical of its mesophilic nature. The ability to thrive at higher temperatures is a desirable trait for algae intended for biofuel production because it opens the possibility of exploiting solar energy in warm, arid regions where water conservation is crucial and land may not be suitable for traditional agriculture (Benemann, 2013; Tiwari et al., 2019). The high-temperature tolerance observed in *C. pacifica* strains and *C. sp.* strain 3222 suggests their suitability for deployment in these environments, where daytime temperatures can limit the productivity of less tolerant species. This advantage could enable continuous, year-round cultivation, contributing to the feasibility of commercial-scale algal biofuel projects in semi-arid and arid regions around the world.

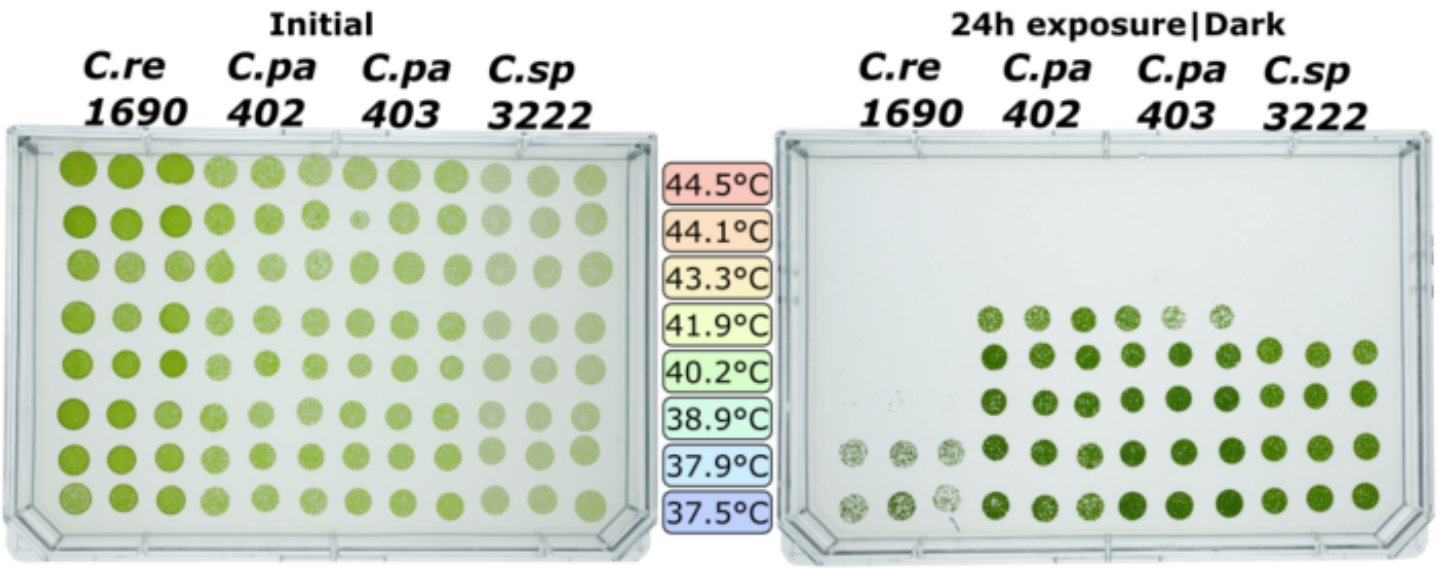

Figure 8: Thermal Tolerance of *Chlamydomonas* Strains in HSM Acetate Media. The left panel shows the initial state of *C. reinhardtii* CC1690, *C. pacifica* strains 402 and 403, and the phylogenetically related *C. sp.* strain 3222 before temperature treatment. The right panel displays the same strains post 24-hour exposure to a

temperature gradient ranging from 37.5°C to 44.5°C, in ascending order from bottom to top, incubated in the dark. The cultures were placed in 100 µL aliquots within a 96-well PCR plate, which was then sealed to ensure containment. Triplicates for each strain and temperature combination were used to ensure experimental reliability. The pattern of growth post-exposure indicates the varying degrees of thermotolerance among the strains, with *C. pacifica* strains and C. sp. strain 3222 exhibiting greater resilience to higher temperatures compared to *C. reinhardtii* CC1690.

Light Tolerance Profile

The investigation into the light tolerance of *Chlamydomonas* strains has elucidated their potential for sustainable growth in high-irradiance environments characteristic of semi-arid regions, where sunlight intensity can be a limiting factor for photosynthetic organisms. In these geographical areas, daily light intensities can frequently surpass 2000 µE/m²·s, demanding high resilience to photic stress for algal survival and productivity (Kirk, 1994; Pruvost et al., 2019). The experimental results demonstrate a stark contrast in light tolerance between the strains: *C. reinhardtii* CC1690 exhibited a clear susceptibility to the light intensity tested, aligning with its natural preference for lower light conditions (**Figure 9**). In contrast, *C. pacifica* strains 402 and 403 and *C. sp.* strain 3222 maintained viability even at high light intensities, indicating a robust photoacclimation capacity that could be highly beneficial for cultivation in regions with intense solar exposure.

This resilience to high light conditions is particularly advantageous in semi-arid regions with intense and consistent solar irradiance. Algae with high light tolerance can utilize abundant sunlight for photosynthesis without the detrimental effects of photoinhibition, thereby maintaining high growth rates and productivity (Cazzaniga et al., 2022; Teoh et al., 2013). This characteristic makes the *C. pacifica* strains and *C. sp.* strain 3222 promising candidates for biofuel and biomass production in such climates, where their ability to thrive could lead to more efficient and sustainable algal farming practices without the competition for arable land typically used for agriculture.

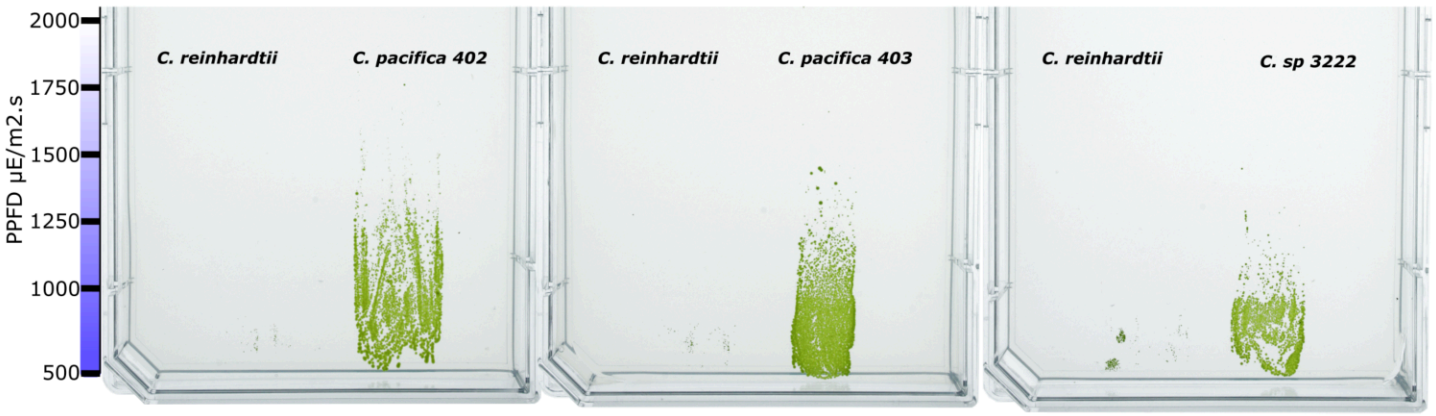

Figure 9: Light Intensity Tolerance of *Chlamydomonas* Strains in HSM Media. The plates demonstrate the growth of *C. reinhardtii* CC1690, *C. pacifica* strains 402 and 403, and *C. sp.* strain 3222 under high light conditions ranging from a minimum of 1000 μE/m²·s to intensities exceeding 2500 μE/m²·s over a period of two days, followed by incubation at 80 μE/m²·s for 5 days. The gradient of light exposure is visually depicted by the diminishing density of algal growth from the bottom (1000 μE/m²·s) to the top of each plate (>2500 μE/m²·s). The comparative analysis highlights the differential tolerance to high light conditions among the strains, with *C. reinhardtii* CC1690 showing notable sensitivity to higher light intensities, while *C. pacifica* strains and *C. sp.* strain 3222 exhibit more robust growth, suggesting a greater resilience to light-induced stress which may confer an advantage in high-light environments.

Motility

The observed motility patterns of *C. pacifica* 402, as depicted in the density graph (**Figure 10; Supplementary Video 1**), indicate the species' adaptive responses to environmental stimuli, highlighting their ecological robustness. The observed range of cell speeds recorded is similar to *C. reinhardtii* with cells reaching 150 μm/s (Molino et al., 2022). The ability to move strategically allows these algae to seek desirable niches for growth and survival, especially in extreme habitats where resources are scarce or conditions are rapidly changing. This characteristic is particularly advantageous for extremophiles that inhabit such environments because motility facilitates the exploitation of microhabitats that provide refuge from extreme stressors or access to nutrients.

From a biotechnological standpoint, the motility of algae like *C. pacifica* 402 can be pivotal in industrial applications. In photobioreactors, for instance, active movement can improve the distribution and exposure of algal cells to light, enhancing photosynthetic efficiency and, consequently, biomass productivity (Martinez Carvajal et al., 2024). In applications such as bioremediation, the mobility of algal cells can be crucial for navigating towards environmental pollutants and crucially aiding in biofilm formation (Singh et al., 2006). Additionally, the motility algae could also be exploited in micromotor drug delivery systems, where extremophile strains could serve as microrobotic platforms to transport drugs to highly acidic gastrointestinal tract (F. Zhang et al., 2022).

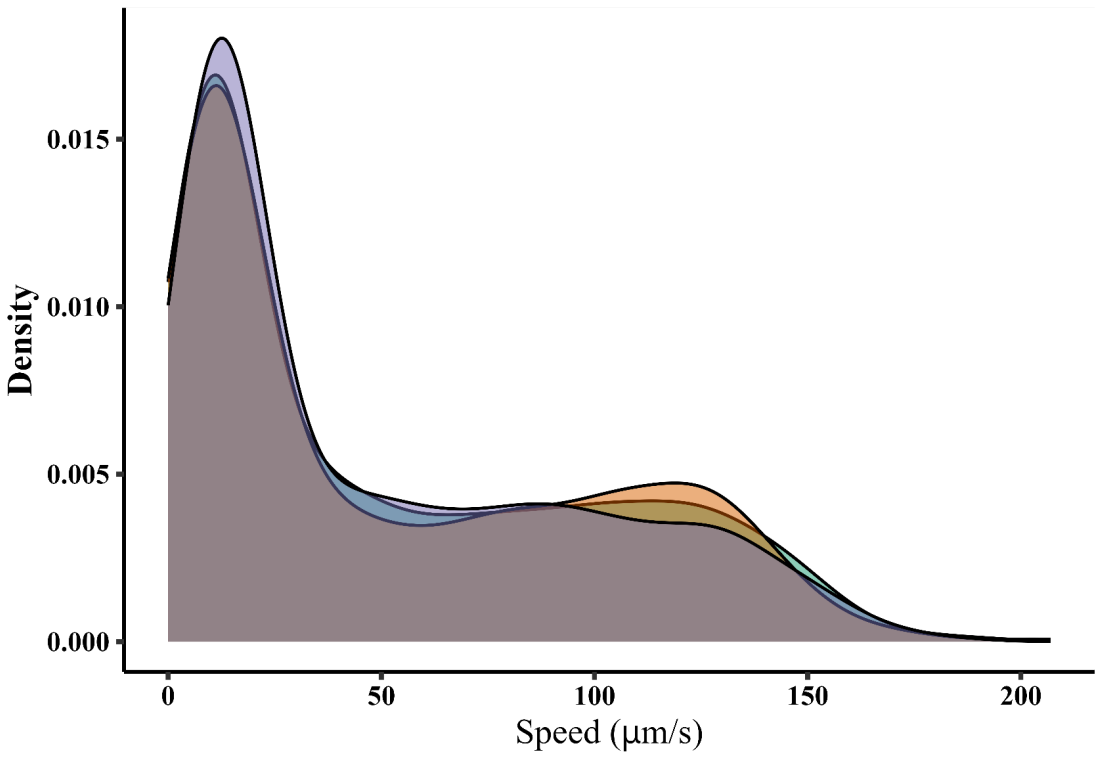

Figure 10: Density Distribution of *C. pacifica* 402 Cell Speed in HSM Media without nitrogen. This graph represents the speed distribution of *C. pacifica* 402 cells, observed under a light microscopy. The density curve suggests a range of cellular speeds observed, with peaks indicating preferred speed ranges, with the fastest cells swimming at 150 µm/s. The plot represents data from three independent biological replicates depicted by each curve.

Recombinant strains

The capacity for genetic manipulation is a cornerstone in utilizing microorganisms for biotechnological applications. The ability to modify and control the genetic makeup of organisms such as algae enables the development of tailored solutions to address a wide array of challenges, from sustainable production of biofuels to environmental remediation. In this context, *Chlamydomonas pacifica* emerges as a promising candidate due to its demonstrated amenability to genetic engineering.

We demonstrate the genetic manipulation of *C. pacifica* (**Figure 11**). As shown in the accompanying images, *C. pacifica* has been successfully modified to express mCherry cytosolic, a red fluorescent protein that allows for the real-time visualization of cellular components and processes (Shaner et al., 2005). Also, we successfully showed the genetic modification of *Chlamydomonas pacifica* strain 403 to secrete PHL7, an enzyme instrumental in the degradation of PET plastics, underscores the remarkable potential of this strain in the field of biotechnology. The clear halos observed around the colonies on selective media highlight the strain's proficiency

in protein secretion, a complex trait that has diverse applications ranging from industrial processing to environmental cleanup (**see Material and Methods**) (Sonnendecker et al., 2021).

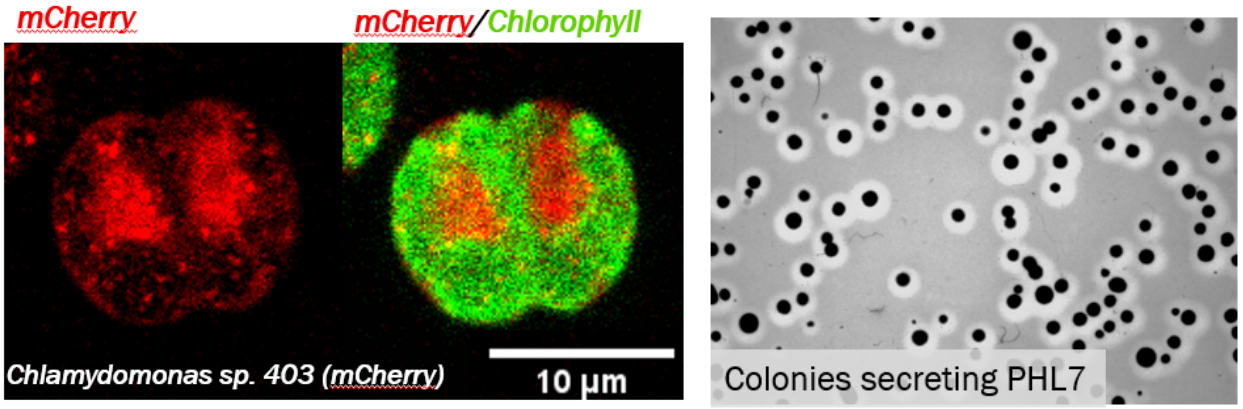

Figure 11: Expression and Secretion Activities of *Chlamydomonas pacifica* 403. The left images display *C. pacifica* 403 cells expressing mCherry, a fluorescent protein, within the cytosol; the first image captures the mCherry fluorescence exclusively and localized in the cytosol, while the second is a composite image showing mCherry overlaid with chlorophyll fluorescence. The red-colored fluorescence of mCherry contrasts with the green-colored chlorophyll, highlighting the expressed protein's subcellular localization. The right image shows a selective HSM acetate agar plate containing zeocin (15 µg/mL) and 0.5% Impranil®, upon which *C. pacifica* 403 colonies have been cultured. The clear halos surrounding the colonies indicate the secretion of PHL7, an enzyme that can degrade PET plastics, demonstrating the strain's potential for biotechnological applications in environmental remediation. The scale bar indicates 10um.

Mating

We observed mating behavior between strains *C. pacifica* 402 and 403 (**Figure 12; Supplementary Video 2 and 3**). The observed mating sequence of *C. pacifica* strains 402 and 403 provides compelling evidence of sexual reproduction capabilities within these algae, a process that plays a crucial ecological role by contributing to genetic diversity and population adaptability (Harris et al., 2009), but also a important tool for breeding specific traits in a single strain (Fields et al., 2019). The detailed imagery begins with presenting a solitary gamete, characterized by its flagella, signifying readiness for mating. As seen in the second image, the subsequent release of the cell wall is an essential prelude to gamete fusion, indicative of the cells' preparation for fusing (Goodenough & Heitman, 2014).

As the process unfolds, initial cell aggregation occurs, a behavior fundamental to the formation of mating pairs, as shown in the third image. This clustering is not merely a physical congregation but a highly regulated event mediated by pheromones and cellular recognition mechanisms (Ferris & Goodenough, 1997). The culmination of

this sequence is the fusion of the mating pair, captured in the fourth image where the fusion channel is evident, establishing a direct conduit for genetic exchange (Harris et al., 2009). This event is a pivotal moment in the sexual life cycle of these organisms and is critical for recombination and the introduction of genetic variability (Colegrave, 2002).

The ability of *C. pacifica* strains to engage in sexual reproduction has profound biotechnological implications. This behavior facilitates breeding programs, allowing for the selection and crossing of strains to combine desirable traits, and would allow improved biofuel production efficiencies or enhanced stress resilience (Fields et al., 2019). The genetic tractability implied by sexual reproduction makes *C. pacifica* an attractive candidate for such programs, as it enables the manipulation of genetic material to achieve targeted improvements in algal strains, which could significantly advance microalgal biotechnology applications.

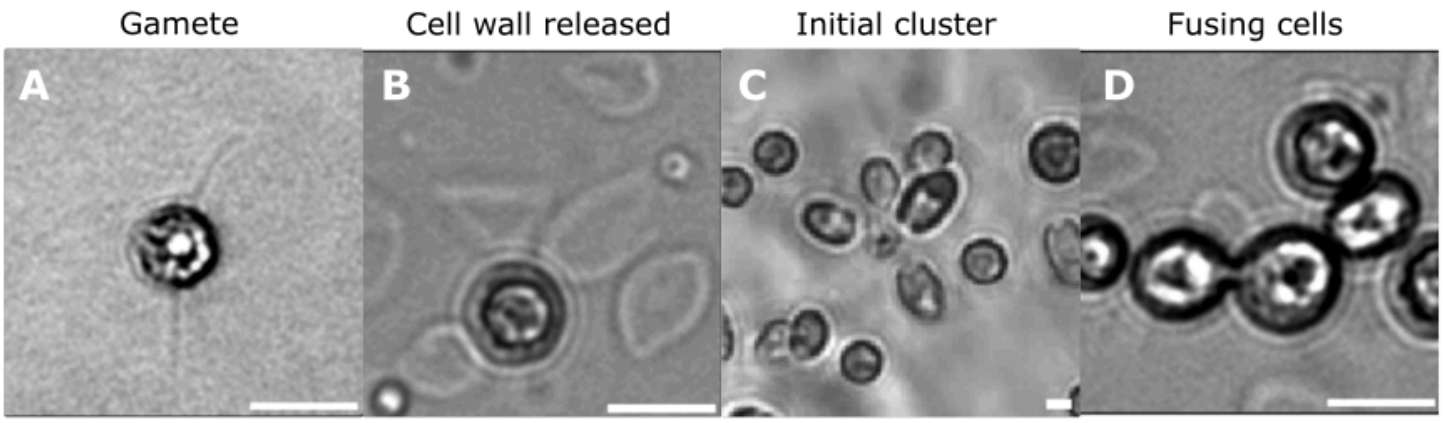

Figure 12: Sequential Stages of Mating in *C. pacifica* Strains 402 and 403. The series of images captures the progressive phases of the mating process. The first image depicts an isolated gamete with flagella ready for mating. The second image shows cells after the release of their cell walls, a preparatory step for gamete fusion. The third image illustrates the initial clustering of cells as they aggregate to form mating pairs. The final image captures a pair of cells in the act of fusion, with the fusion channel visibly formed between them, facilitating the exchange of genetic material. This sequence of events underscores the complex mating behavior exhibited by these algae and provides a visual representation of sexual reproduction in *Chlamydomonas* species. Scale bar indicates 10 um.

In this study, we present further evidence of the successful mating between *Chlamydomonas pacifica* strains 402 and 403, reinforcing the sexual reproduction capabilities within these algal strains. The image captured post-mating shows progeny colonies growing on a selective medium containing hygromycin (30 µg/mL) and zeocin (15 µg/mL), supplemented with 0.5% Impranil (**Figure 13**). The dual resistance to both antibiotics in the progeny is a definitive indication of genetic material exchange between the two parent strains, as each parent harbored a distinct resistance marker: strain 402 contained the pJPSHx1PHL7 vector for hygromycin resistance,

and strain 403 carried the pAH04mCherry vector for zeocin resistance. The survival and growth of these progeny colonies under stringent selection conditions corroborate the mating event and confirm the inheritance and functional expression of both antibiotic resistance genes and the PHL7 secretion phenotype from the parental strains. This demonstrates the successful combination of genetic traits through sexual reproduction, which is a powerful tool for strain improvement and has profound implications for algal biotechnology (Fields et al., 2019). These results highlight the potential of *C. pacifica* strains for use in biotechnological applications that require complex genetic manipulations, such as developing strains for bioremediation purposes or producing value-added compounds. Moreover, the ability to secrete enzymes like PHL7 underscores the potential for these algae to contribute to environmental sustainability, particularly in the degradation of persistent pollutants such as PET plastics (Sonnendecker et al., 2021).

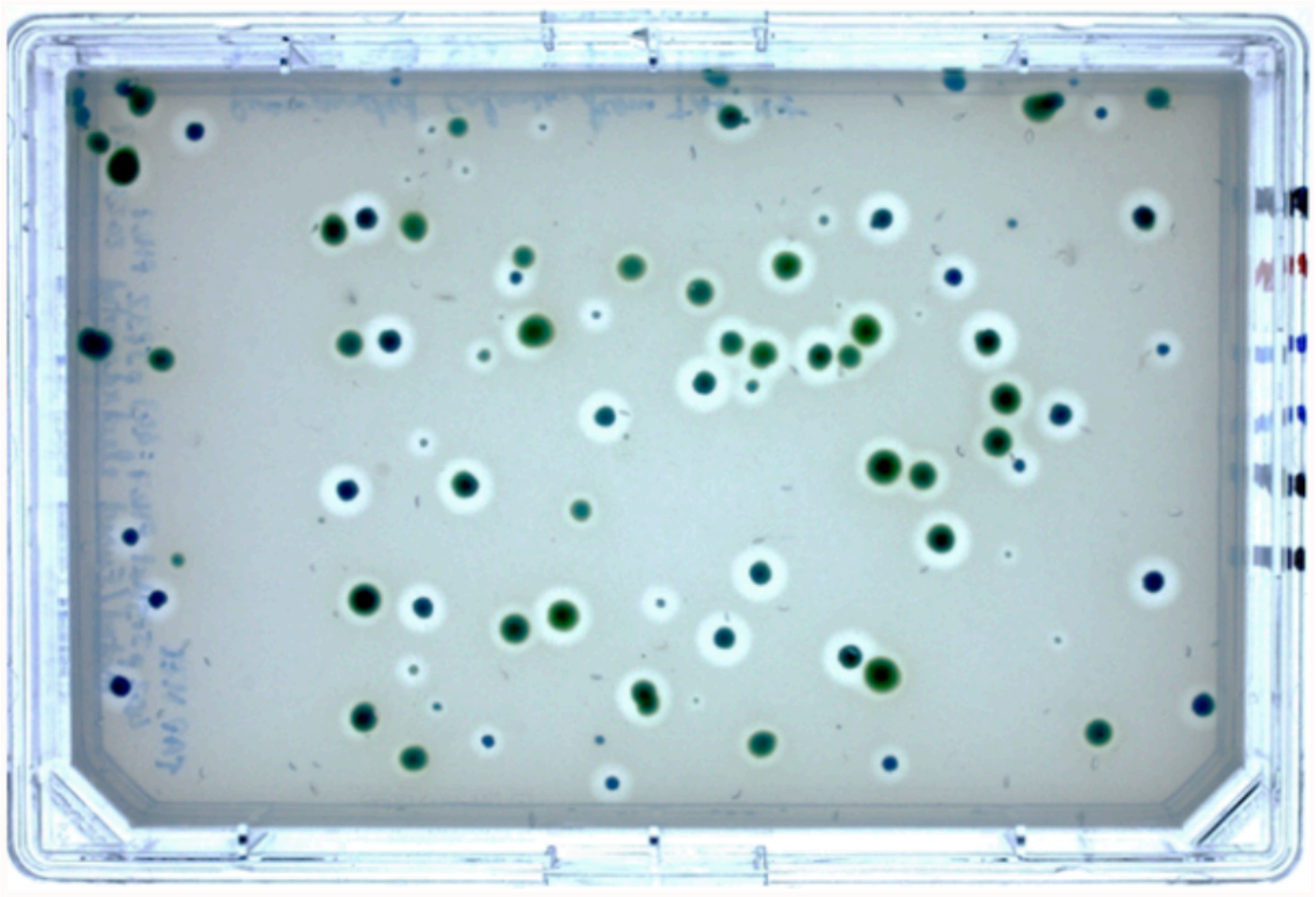

Figure 13: Selection of Progeny from Mating of *Chlamydomonas pacifica* Strains 402 (Hygromycin Resistant) and 403 (Zeocin Resistant). This image showcases the progeny resulting from the mating of *C. pacifica* 402, which harbors the pJPSHx1PHL7 vector conferring hygromycin resistance and the ability to secrete PHL7, with *C. pacifica* 403, carrier of the pAH04mCherry vector that confers zeocin resistance and encodes for cytosolic expression of mCherry. The selection plate contains hygromycin (30 µg/mL) and zeocin (15 µg/mL),

along with 0.5% Impranil, ensuring that only progeny inheriting both resistance genes and the associated PHL7 secretion capability survive. The presence of green colonies amidst the selective agents indicates successful mating and genetic exchange between the two strains, leading to a new generation of algae with combined traits for antibiotic resistance and enzymatic activity.

Lipidomics

We performed a comprehensive lipidomic profile of *C. pacifica*, derived from both negative and positive ionization modes of mass spectrometry (**Table 1 and 2**). These tables encapsulate the diverse lipid species detected within the algal strain, with a rich array of triacylglycerols (TAGs) pertinent to biofuel applications. Additionally, we observed some relevant nutraceuticals and dietary supplements, given the health-promoting potential of the fatty acids identified in these lipid classes. We further discuss each possible application below.

Triacylglycerol Composition and Biofuel Potential

Lipidomic analysis of *C. pacifica*, utilizing both positive and negative ionization modes, has revealed a lipid profile rich in triacylglycerols (TAGs), which are particularly interesting for biofuel applications. Specifically, the positive ionization mode data elucidated a series of TAGs (circa 20%), comprising glycerol bound to three fatty acids, making them highly reduced forms of carbon and, thus, energy-dense molecules suitable for biofuel production (**Table 1 and 2**).

Among the detected TAGs, TAG (16:0/18:2(9Z,12Z)/18:3(9Z,12Z,15Z))[iso6] and TAG(16:0/18:1(9Z)/18:3(9Z,12Z,15Z))[iso6] stand out due to their fatty acid composition. The presence of fatty acids with chain lengths of 16 and 18 carbons, including unsaturated versions like 18:2 (linoleic acid) and 18:3 (α-linolenic acid), is promising for biodiesel quality. These fatty acids contribute to biodiesel's cold flow properties and oxidative stability, which are crucial parameters for fuel performance and shelf-life (Knothe, 2005). As a starting point, *C. pacifica* can be improved to maximize lipid yield and the extraction process enhanced to improve economic feasibility of biofuel production. Additionally, metabolic engineering strategies could increase the proportion of desirable fatty acids, such as increasing the saturation level to improve biodiesel stability or tweaking the carbon chain length to favor biodiesel properties (Ibáñez-Salazar et al., 2014; Lu et al., 2008).

Fatty Acid Composition and Health-Promoting Potential

The comprehensive lipidomic profile of *C. pacifica* has uncovered a spectrum of lipid species with significant potential for nutraceuticals and dietary supplements. Notably, the analysis identified an array of TAGs and phospholipids with fatty acid compositions that benefit human health (**Table 1 and 2**). Among the lipid compounds identified, the presence of TAGs containing omega-3 and omega-6 fatty acids, such as linoleic acid

(18:2) and α-linolenic acid (18:3) (**Table 2**), is particularly noteworthy. These polyunsaturated fatty acids (PUFAs) are essential components of the human diet as well, as they are precursors to eicosapentaenoic acid (EPA) and docosahexaenoic acid (DHA), which play critical roles in maintaining cardiovascular health and cognitive function (Swanson et al., 2012). The analysis also revealed phospholipids like phosphatidylcholines (PCs) and phosphatidylinositols (PIs) (**Table 1**), which are integral to cell membrane structure and have been associated with health benefits, including liver health and cognitive improvements (Küllenberg et al., 2012).

The identification of these lipid classes in *C. pacifica* offers exciting possibilities for the development of algae-based nutraceuticals and dietary supplements. The cultivation of microalgae as a source of PUFAs and other bioactive lipids is a growing area of interest due to the sustainability of algae as a resource and the potential health benefits they offer (Diaz et al., 2023).

Table 1: Lipidomic profile of *Chlamydomonas pacifica*: identification, classification, and relative abundance of lipid species in negative mode analysis.

Description	Class	Formula	Relative (%)
PC(18:3(6Z,9Z,12Z)/LTE4)	PC	C49H83N2O11PS	13.81
Similar to Chlorophyll a	Tetrapyrroles	C55H72MgN4O5	10.55
Similar to PI (18:0/5-iso PGF2VI)	PI	C45H81O16P	3.65
Digalactosyldiacylglycerol	Glycerolipids	C49H88O15	3.48
Similar toChlorophyll a	Tetrapyrroles	C55H72MgN4O5	3.31
MGDG 18:3_16:4	MGDG	C43H68O10	3.26
PG(18:1(9Z)/20:4(5Z,8Z,11Z,14Z))	PG	C44H77O10P	2.47
MGDG(18:3(9Z,12Z,15Z)/16:3(7Z,10Z,13Z))	MGDG	C43H70O10	2.46
PG(18:2(9Z,12Z)/16:1(9Z))	PG	C40H73O10P	2.44
PI(18:2(9Z,12Z)/22:0)	PI	C49H91O13P	1.87
PI(PGF1alpha/16:2(9Z,12Z))	PI	C45H79O16P	1.49
DGDG 18:1_16:3	DGDG	C49H84O15	1.32

PI(16:0/18:1(9Z))	PI	C43H81O13P	1.26
Similar toPI(18:0/5-iso PGF2VI)	PI	C45H81O16P	1.18
DGTS(16:0/18:2(9Z,12Z))	DGTS	C44H81NO7	1.17
unknown	-	-	14.97

Table 2: Lipidomic profile of *Chlamydomonas pacifica*: identification, classification, and relative abundance of lipid species in positive mode analysis.

Description	Class	Formula	Relative (%)
Chlorophyll a	Tetrapyrroles	C55H72MgN4O5	6.59
TAG(16:0/18:2(9Z,12Z)/18:3(9Z,12Z,15Z))[iso6]	TAG	C55H96O6	2.64
TAG(16:0/18:1(9Z)/18:3(9Z,12Z,15Z))[iso6]	TAG	C55H98O6	2.48
GalCer(d18:2/20:1)	GalCer	C44H81NO8	2.24
TAG(16:0/18:0/18:2(9Z,12Z))[iso6]	TAG	C55H102O6	2.07
DGTS(16:0/18:2(9Z,12Z))	DGTS	C44H81NO7	1.97
Similar to TG(16:0/18:1(9Z)/18:2(9Z,12Z))[iso6]	TG	C55H100O6	1.89
PA(22:5(7Z,10Z,13Z,16Z,19Z)/18:3(6Z,9Z,12Z))	PA	C43H69O8P	1.69
TAG(16:0/17:2(9Z,12Z)/17:2(9Z,12Z))[iso3]	TAG	C53H94O6	1.56
Glycerol 2-(9Z,12Z-octadecadienoate) 1-hexadecanoate 3-O-[alpha-D-galactopyranosyl-(1->6)-beta-D-galactopyranoside]	Glycerolipids	C49H88O15	1.47
Similar to MGDG(18:3(9Z,12Z,15Z)/16:3(7Z,10Z,13Z))	MGDG	C43H70O10	1.42
TAG(16:0/16:1(9Z)/18:2(9Z,12Z))[iso6]	TAG	C53H96O6	1.35

GalCer(d18:1/20:0)	GalCer	C44H85NO8	1.25
Similar to 1-(6-[3]-ladderane-hexanyl)-2-(8-[3]-ladderane-octanyl)-sn-glycerophosphocholine	PC	C46H80NO6P	1.24
unknown	-	-	9.37

Conclusion

Based on the comprehensive multi-omics, including genomics, metabolomics, and lipidomics, analysis of the extremophile alga *C. pacifica*, our findings underscore its remarkable versatility and robustness, marking it as a significant organism for biotechnological applications. The study demonstrates *C. pacifica*'s efficient nitrogen and carbon assimilation abilities, high tolerance to pH and salinity, and resilience under various light and temperature conditions. The mating capacity between strains 402 and 403, along with the proven potential for genetic manipulation, exemplifies the organism's suitability for advanced biotechnological processes, and strategies to manipulate and improve the strain to different goals. These traits, coupled with the alga's genetic tractability, present *C. pacifica* as an excellent candidate for future metabolic engineering endeavors aimed at sustainable biotechnological solutions.

Conflict of Interest

SM is a co-founder and equity holder in Algenesis Inc., a company that might gain from the outcomes of this research. The other authors affirm that their research was carried out without any commercial or financial ties that could be perceived as a potential conflict of interest.

Authors Contributions

JVDM: Conceptualization, Data curation, Formal analysis, Investigation, Methodology, Visualization, Writing – original draft, Writing – review & editing
AO: Data curation, Formal analysis, Software, Visualization, Writing – review & editing
HS: Data curation, Formal analysis, Software, Visualization, Writing – review & editing
KK: Investigation, Methodology, Visualization, Writing – review & editing
BS: Investigation, Methodology, Writing – review & editing

CJD: Investigation, Writing – review & editing
AG: Data curation, Investigation, Formal analysis, Software, Visualization, Writing – review & editing
LJJ: Investigation, Writing – review & editing
YT-T: Writing – review & editing
NH: Investigation, Writing – review & editing
AB: Investigation, Writing – review & editing
HJ: Investigation, Writing – review & editing
FF: Investigation, Writing – review & editing
SM: contributed to drafting and revising the original manuscript and secured funding for the research.

Funding

This work is supported by the U.S. Department of Energy's Office of Energy Efficiency and Renewable Energy (EERE) under the APEX award number DE-EE0009671.

Acknowledgment

The authors thank Jennifer Santini and Marcy Erb (UCSD School of Medicine Microscopy Core, supported by NINDS P30NS047101 grant) for help with confocal microscopy. This publication includes data generated at the UC San Diego IGM Genomics Center utilizing an Illumina NovaSeq 6000 that was purchased with funding from a National Institutes of Health SIG grant (#S10 OD026929). The lipidomics data were generated at the Metabolomics Core facility at the University of California, Riverside. Icon made by Pixel perfect, Freepik and Uniconlabs from www.flaticon.com.

References

Abdelfattah, A., Ali, S. S., Ramadan, H., El-Aswar, E. I., Eltawab, R., Ho, S.-H., Elsamahy, T., Li, S., El-Sheekh, M. M., Schagerl, M., Kornaros, M., & Sun, J. (2023). Microalgae-based wastewater treatment: Mechanisms, challenges, recent advances, and future prospects. *Environmental Science and Ecotechnology*, *13*, 100205. https://doi.org/10.1016/j.ese.2022.100205

Ahmad, A., & Ashraf, S. S. (2023). Sustainable food and feed sources from microalgae: Food security and the circular bioeconomy. *Algal Research*, *74*, 103185. https://doi.org/10.1016/j.algal.2023.103185

Altschul, S. F., Gish, W., Miller, W., Myers, E. W., & Lipman, D. J. (1990). Basic local alignment search

tool. *Journal of Molecular Biology*, *215*(3), 403–410. https://doi.org/10.1016/S0022-2836(05)80360-2

Benemann, J. (2013). Microalgae for Biofuels and Animal Feeds. *Energies*, *6*(11), Article 11. https://doi.org/10.3390/en6115869

Bogaert, K. A., Perez, E., Rumin, J., Giltay, A., Carone, M., Coosemans, N., Radoux, M., Eppe, G., Levine, R. D., Remacle, F., & Remacle, C. (2019). Metabolic, Physiological, and Transcriptomics Analysis of Batch Cultures of the Green Microalga Chlamydomonas Grown on Different Acetate Concentrations. *Cells*, *8*(11), Article 11. https://doi.org/10.3390/cells8111367

Brock, T. D. (1975). Salinity and the Ecology of Dunaliella from Great Salt Lake. *Microbiology*, *89*(2), 285–292. https://doi.org/10.1099/00221287-89-2-285

Cantalapiedra, C. P., Hernández-Plaza, A., Letunic, I., Bork, P., & Huerta-Cepas, J. (2021). eggNOG-mapper v2: Functional Annotation, Orthology Assignments, and Domain Prediction at the Metagenomic Scale. *Molecular Biology and Evolution*, *38*(12), 5825–5829. https://doi.org/10.1093/molbev/msab293

Cazzaniga, S., Perozeni, F., Baier, T., & Ballottari, M. (2022). Engineering astaxanthin accumulation reduces photoinhibition and increases biomass productivity under high light in Chlamydomonas reinhardtii. *Biotechnology for Biofuels and Bioproducts*, *15*(1), 77. https://doi.org/10.1186/s13068-022-02173-3

Chen, S., Zhou, Y., Chen, Y., & Gu, J. (2018). fastp: An ultra-fast all-in-one FASTQ preprocessor. *Bioinformatics*, *34*(17), i884–i890. https://doi.org/10.1093/bioinformatics/bty560

Colegrave, N. (2002). Sex releases the speed limit on evolution. *Nature*, *420*(6916), 664–666. https://doi.org/10.1038/nature01191

Craig, R. J., Gallaher, S. D., Shu, S., Salomé, P. A., Jenkins, J. W., Blaby-Haas, C. E., Purvine, S. O., O'Donnell, S., Barry, K., Grimwood, J., Strenkert, D., Kropat, J., Daum, C., Yoshinaga, Y., Goodstein, D. M., Vallon, O., Schmutz, J., & Merchant, S. S. (2022). The Chlamydomonas Genome Project, version 6: Reference assemblies for mating-type plus and minus strains reveal extensive structural mutation in the laboratory. *The Plant Cell*, *35*(2), 644–672. https://doi.org/10.1093/plcell/koac347

Delwiche, C. F., & Cooper, E. D. (2015). The Evolutionary Origin of a Terrestrial Flora. *Current Biology*, *25*(19), R899–R910. https://doi.org/10.1016/j.cub.2015.08.029

Dhaliwal, G., Lee, T., Talwar, D., & Wang, O. (2017). Effect of varying pH adjusted media on the growth rate of Chlamydomonas reinhardtii. *The Expedition*, *7*. https://ojs.library.ubc.ca/index.php/expedition/article/view/190221

Diaz, C. J., Douglas, K. J., Kang, K., Kolarik, A. L., Malinovski, R., Torres-Tiji, Y., Molino, J. V., Badary, A., & Mayfield, S. P. (2023). Developing algae as a sustainable food source. *Frontiers in Nutrition*, *9*. https://www.frontiersin.org/articles/10.3389/fnut.2022.1029841

Dobin, A., Davis, C. A., Schlesinger, F., Drenkow, J., Zaleski, C., Jha, S., Batut, P., Chaisson, M., & Gingeras, T. R. (2013). STAR: Ultrafast universal RNA-seq aligner. *Bioinformatics*, *29*(1), 15–21. https://doi.org/10.1093/bioinformatics/bts635

Edgar, R. C. (2004). MUSCLE: A multiple sequence alignment method with reduced time and space complexity. *BMC Bioinformatics*, *5*(1), 113. https://doi.org/10.1186/1471-2105-5-113

Ejike, C. E. C. C., Ezeorba, T. P. C., Ajah, O., & Udenigwe, C. C. (2023). Big Things, Small Packages: An Update on Microalgae as Sustainable Sources of Nutraceutical Peptides for Promoting Cardiovascular Health. *Global Challenges*, *7*(5), 2200162. https://doi.org/10.1002/gch2.202200162

Erickson, E., Wakao, S., & Niyogi, K. K. (2015). Light stress and photoprotection in Chlamydomonas reinhardtii. *The Plant Journal*, *82*(3), 449–465. https://doi.org/10.1111/tpj.12825

Fernández, E., Llamas, Á., & Galván, A. (2009). Chapter 3—Nitrogen Assimilation and its Regulation. In E. H. Harris, D. B. Stern, & G. B. Witman (Eds.), *The Chlamydomonas Sourcebook (Second Edition)* (pp. 69–113). Academic Press. https://doi.org/10.1016/B978-0-12-370873-1.00011-3

Ferris, P. J., Armbrust, E. V., & Goodenough, U. W. (2002). Genetic Structure of the Mating-Type Locus of Chlamydomonas reinhardtii. *Genetics*, *160*(1), 181–200. https://doi.org/10.1093/genetics/160.1.181

Ferris, P. J., & Goodenough, U. W. (1997). Mating Type in Chlamydomonas Is Specified by mid, the Minus-Dominance Gene. *Genetics*, *146*(3), 859–869. https://doi.org/10.1093/genetics/146.3.859

Fields, F. J., Ostrand, J. T., Tran, M., & Mayfield, S. P. (2019). Nuclear genome shuffling significantly

increases production of chloroplast-based recombinant protein in Chlamydomonas reinhardtii. *Algal Research*, *41*(February). https://doi.org/10.1016/j.algal.2019.101523

Gabriel, L., Brůna, T., Hoff, K. J., Ebel, M., Lomsadze, A., Borodovsky, M., & Stanke, M. (2024). BRAKER3: Fully automated genome annotation using RNA-seq and protein evidence with GeneMark-ETP, AUGUSTUS, and TSEBRA. *Genome Research*, *34*(5), 769–777. https://doi.org/10.1101/gr.278090.123

Goodenough, U., & Heitman, J. (2014). Origins of Eukaryotic Sexual Reproduction. *Cold Spring Harbor Perspectives in Biology*, *6*(3), a016154. https://doi.org/10.1101/cshperspect.a016154

Harris, E. H., Stern, D. B., & Witman, G. B. (Eds.). (2009). Chapter 5—The Sexual Cycle. In *The Chlamydomonas Sourcebook (Second Edition)* (pp. 119–157). Academic Press. https://doi.org/10.1016/B978-0-12-370873-1.00005-8

Hoff, K. J., & Stanke, M. (2019). Predicting Genes in Single Genomes with AUGUSTUS. *Current Protocols in Bioinformatics*, *65*(1), e57. https://doi.org/10.1002/cpbi.57

Hollin, T., Abel, S., Falla, A., Pasaje, C. F. A., Bhatia, A., Hur, M., Kirkwood, J. S., Saraf, A., Prudhomme, J., De Souza, A., Florens, L., Niles, J. C., & Le Roch, K. G. (2022). Functional genomics of RAP proteins and their role in mitoribosome regulation in Plasmodium falciparum. *Nature Communications*, *13*(1), Article 1. https://doi.org/10.1038/s41467-022-28981-7

Huerta-Cepas, J., Szklarczyk, D., Heller, D., Hernández-Plaza, A., Forslund, S. K., Cook, H., Mende, D. R., Letunic, I., Rattei, T., Jensen, L. J., von Mering, C., & Bork, P. (2019). eggNOG 5.0: A hierarchical, functionally and phylogenetically annotated orthology resource based on 5090 organisms and 2502 viruses. *Nucleic Acids Research*, *47*(D1), D309–D314. https://doi.org/10.1093/nar/gky1085

Ibáñez-Salazar, A., Rosales-Mendoza, S., Rocha-Uribe, A., Ramírez-Alonso, J. I., Lara-Hernández, I., Hernández-Torres, A., Paz-Maldonado, L. M. T., Silva-Ramírez, A. S., Bañuelos-Hernández, B., Martínez-Salgado, J. L., & Soria-Guerra, R. E. (2014). Over-expression of Dof-type transcription factor increases lipid production in Chlamydomonas reinhardtii. *Journal of Biotechnology*, *184*, 27–38. https://doi.org/10.1016/j.jbiotec.2014.05.003

Johnson, M., Zaretskaya, I., Raytselis, Y., Merezhuk, Y., McGinnis, S., & Madden, T. L. (2008). NCBI

BLAST: A better web interface. *Nucleic Acids Research*, *36*(Web Server issue), W5-9. https://doi.org/10.1093/nar/gkn201

Kirk, J. T. O. (1994). *Light and Photosynthesis in Aquatic Ecosystems* (2nd ed.). Cambridge University Press. https://doi.org/10.1017/CBO9780511623370

Knothe, G. (2005). Dependence of biodiesel fuel properties on the structure of fatty acid alkyl esters. *Fuel Processing Technology*, *86*(10), 1059–1070. https://doi.org/10.1016/j.fuproc.2004.11.002

Kolmogorov, M., Yuan, J., Lin, Y., & Pevzner, P. A. (2019). Assembly of long, error-prone reads using repeat graphs. *Nature Biotechnology*, *37*(5), Article 5. https://doi.org/10.1038/s41587-019-0072-8

Kubo, T., Saito, T., Fukuzawa, H., & Matsuda, Y. (2001). Two tandemly-located matrix metalloprotease genes with different expression patterns in the Chlamydomonas sexual cell cycle. *Current Genetics*, *40*(2), 136–143. https://doi.org/10.1007/s002940100239

Küllenberg, D., Taylor, L. A., Schneider, M., & Massing, U. (2012). Health effects of dietary phospholipids. *Lipids in Health and Disease*, *11*(1), 3. https://doi.org/10.1186/1476-511X-11-3

Kumar, G., Shekh, A., Jakhu, S., Sharma, Y., Kapoor, R., & Sharma, T. R. (2020). Bioengineering of Microalgae: Recent Advances, Perspectives, and Regulatory Challenges for Industrial Application. *Frontiers in Bioengineering and Biotechnology*, *8*. https://doi.org/10.3389/fbioe.2020.00914

Kuznetsov, D., Tegenfeldt, F., Manni, M., Seppey, M., Berkeley, M., Kriventseva, E. V., & Zdobnov, E. M. (2023). OrthoDB v11: Annotation of orthologs in the widest sampling of organismal diversity. *Nucleic Acids Research*, *51*(D1), D445–D451. https://doi.org/10.1093/nar/gkac998

Larkin, M. A., Blackshields, G., Brown, N. P., Chenna, R., McGettigan, P. A., McWilliam, H., Valentin, F., Wallace, I. M., Wilm, A., Lopez, R., Thompson, J. D., Gibson, T. J., & Higgins, D. G. (2007). Clustal W and Clustal X version 2.0. *Bioinformatics*, *23*(21), 2947–2948. https://doi.org/10.1093/bioinformatics/btm404

Lin, H., & Goodenough, U. W. (2007). Gametogenesis in the Chlamydomonas reinhardtii minus Mating Type Is Controlled by Two Genes, MID and MTD1. *Genetics*, *176*(2), 913–925. https://doi.org/10.1534/genetics.106.066167

Liu, J., He, J., Xue, R., Xu, B., Qian, X., Xin, F., Blank, L. M., Zhou, J., Wei, R., Dong, W., & Jiang, M.

(2021). Biodegradation and up-cycling of polyurethanes: Progress, challenges, and prospects. *Biotechnology Advances*, *48*, 107730. https://doi.org/10.1016/j.biotechadv.2021.107730

Lu, X., Vora, H., & Khosla, C. (2008). Overproduction of free fatty acids in E. coli: Implications for biodiesel production. *Metabolic Engineering*, *10*(6), 333–339. https://doi.org/10.1016/j.ymben.2008.08.006

Luís, A. T., Córdoba, F., Antunes, C., Loayza-Muro, R., Grande, J. A., Silva, B., Diaz-Curiel, J., & Ferreira da Silva, E. (2022). Extremely Acidic Eukaryotic (Micro) Organisms: Life in Acid Mine Drainage Polluted Environments—Mini-Review. *International Journal of Environmental Research and Public Health*, *19*(1), Article 1. https://doi.org/10.3390/ijerph19010376

Mackinder, L. C. M., Meyer, M. T., Mettler-Altmann, T., Chen, V. K., Mitchell, M. C., Caspari, O., Freeman Rosenzweig, E. S., Pallesen, L., Reeves, G., Itakura, A., Roth, R., Sommer, F., Geimer, S., Mühlhaus, T., Schroda, M., Goodenough, U., Stitt, M., Griffiths, H., & Jonikas, M. C. (2016). A repeat protein links Rubisco to form the eukaryotic carbon-concentrating organelle. *Proceedings of the National Academy of Sciences*, *113*(21), 5958–5963. https://doi.org/10.1073/pnas.1522866113

Manni, M., Berkeley, M. R., Seppey, M., Simão, F. A., & Zdobnov, E. M. (2021). BUSCO Update: Novel and Streamlined Workflows along with Broader and Deeper Phylogenetic Coverage for Scoring of Eukaryotic, Prokaryotic, and Viral Genomes. *Molecular Biology and Evolution*, *38*(10), 4647–4654. https://doi.org/10.1093/molbev/msab199

Martinez Carvajal, G. D., Taidi, B., & Jarrahi, M. (2024). Towards a low energy, stirless photobioreactor using photosynthetic motile microalgae. *Algal Research*, *77*, 103350. https://doi.org/10.1016/j.algal.2023.103350

Masi, A., Leonelli, F., Scognamiglio, V., Gasperuzzo, G., Antonacci, A., & Terzidis, M. A. (2023). Chlamydomonas reinhardtii: A Factory of Nutraceutical and Food Supplements for Human Health. *Molecules (Basel, Switzerland)*, *28*(3), 1185. https://doi.org/10.3390/molecules28031185

McGowen, J. A. (2019). *The Algae Testbed Public Private Partnership -ATP3 (Final Closeout Report)* (DOE-ASU-ATP3-Final). Arizona State Univ., Tempe, AZ (United States). https://doi.org/10.2172/1780639

Melack, J. M. (1979). Photosynthesis and growth of Spirulina platensis (Cyanophyta) in an equatorial lake (Lake Simbi, Kenya). *Limnology and Oceanography*, *24*(4), 753–760. https://doi.org/10.4319/lo.1979.24.4.0753

Milo, R., Jorgensen, P., Moran, U., Weber, G., & Springer, M. (2010). BioNumbers—The database of key numbers in molecular and cell biology. *Nucleic Acids Research*, *38*(suppl_1), D750–D753. https://doi.org/10.1093/nar/gkp889

Molino, J. V. D., Carpine, R., Gademann, K., Mayfield, S., & Sieber, S. (2022). Development of a cell surface display system in Chlamydomonas reinhardtii. *Algal Research*, *61*, 102570–102570. https://doi.org/10.1016/j.algal.2021.102570

Molino, J. V. D., de Carvalho, J. C. M., Mayfield, S. P., Carvalho, J. C. M., & Mayfield, S. P. (2018). Comparison of secretory signal peptides for heterologous protein expression in microalgae: Expanding the secretion portfolio for Chlamydomonas reinhardtii. *PLoS ONE*, *13*(2), 1–20. https://doi.org/10.1371/journal

Nelson, D. R., Chaiboonchoe, A., Fu, W., Hazzouri, K. M., Huang, Z., Jaiswal, A., Daakour, S., Mystikou, A., Arnoux, M., Sultana, M., & Salehi-Ashtiani, K. (2019). Potential for Heightened Sulfur-Metabolic Capacity in Coastal Subtropical Microalgae. *iScience*, *11*, 450–465. https://doi.org/10.1016/j.isci.2018.12.035

Ning, J., Otto, T. D., Pfander, C., Schwach, F., Brochet, M., Bushell, E., Goulding, D., Sanders, M., Lefebvre, P. A., Pei, J., Grishin, N. V., Vanderlaan, G., Billker, O., & Snell, W. J. (2013). Comparative genomics in Chlamydomonas and Plasmodium identifies an ancient nuclear envelope protein family essential for sexual reproduction in protists, fungi, plants, and vertebrates. *Genes & Development*, *27*(10), 1198–1215. https://doi.org/10.1101/gad.212746.112

Novoveská, L., Nielsen, S. L., Eroldoğan, O. T., Haznedaroglu, B. Z., Rinkevich, B., Fazi, S., Robbens, J., Vasquez, M., & Einarsson, H. (2023). Overview and Challenges of Large-Scale Cultivation of Photosynthetic Microalgae and Cyanobacteria. *Marine Drugs*, *21*(8), Article 8. https://doi.org/10.3390/md21080445

Oren, A. (2014). The ecology of Dunaliella in high-salt environments. *Journal of Biological Research-Thessaloniki*, *21*(1), 23. https://doi.org/10.1186/s40709-014-0023-y

Pinello, J. F., & Clark, T. G. (2022). HAP2-Mediated Gamete Fusion: Lessons From the World of Unicellular Eukaryotes. *Frontiers in Cell and Developmental Biology*, *9*, 807313. https://doi.org/10.3389/fcell.2021.807313

Pruvost, J., Goetz, V., Artu, A., Das, P., & Al Jabri, H. (2019). Thermal modeling and optimization of microalgal biomass production in the harsh desert conditions of State of Qatar. *Algal Research*, *38*, 101381. https://doi.org/10.1016/j.algal.2018.12.006

Remias, D., Lütz-Meindl, U., & Lütz, C. (2005). Photosynthesis, pigments and ultrastructure of the alpine snow alga Chlamydomonas nivalis. *European Journal of Phycology*, *40*(3), 259–268. https://doi.org/10.1080/09670260500202148

Ren, C.-G., Liu, Z.-Y., Zhong, Z.-H., Wang, X.-L., & Qin, S. (2022). Integrated biotechnology to mitigate green tides. *Environmental Pollution*, *309*, 119764. https://doi.org/10.1016/j.envpol.2022.119764

Selvaratnam, T., Pegallapati, A. K., Montelya, F., Rodriguez, G., Nirmalakhandan, N., Van Voorhies, W., & Lammers, P. J. (2014). Evaluation of a thermo-tolerant acidophilic alga, *Galdieria sulphuraria*, for nutrient removal from urban wastewaters. *Bioresource Technology*, *156*, 395–399. https://doi.org/10.1016/j.biortech.2014.01.075

Seppey, M., Manni, M., & Zdobnov, E. M. (2019). BUSCO: Assessing Genome Assembly and Annotation Completeness. In M. Kollmar (Ed.), *Gene Prediction: Methods and Protocols* (pp. 227–245). Springer. https://doi.org/10.1007/978-1-4939-9173-0_14

Shaner, N. C., Steinbach, P. A., & Tsien, R. Y. (2005). A guide to choosing fluorescent proteins. *Nature Methods*, *2*(12), 905–909. https://doi.org/10.1038/NMETH819

Singh, R., Paul, D., & Jain, R. K. (2006). Biofilms: Implications in bioremediation. *Trends in Microbiology*, *14*(9), 389–397. https://doi.org/10.1016/j.tim.2006.07.001

Sonnendecker, C., Oeser, J., Richter, P. K., Hille, P., Zhao, Z., Fischer, C., Lippold, H., Blázquez-Sánchez, P., Engelberger, F., Ramírez-Sarmiento, C. A., Oeser, T., Lihanova, Y., Frank, R., Jahnke, H.-G., Billig, S., Abel, B., Sträter, N., Matysik, J., & Zimmermann, W. (2021). Low Carbon Footprint Recycling of Post-Consumer PET Plastic with a Metagenomic Polyester Hydrolase. *ChemSusChem*. https://doi.org/10.1002/cssc.202101062

Stanton, J. S., Anning, D. W., Brown, C. J., Moore, R. B., McGuire, V. L., Qi, S. L., Harris, A. C.,

Dennehy, K. F., McMahon, P. B., Degnan, J. R., & Böhlke, J. K. (2017). Brackish groundwater in the United States. In *Professional Paper* (1833). U.S. Geological Survey. https://doi.org/10.3133/pp1833

Swanson, D., Block, R., & Mousa, S. A. (2012). Omega-3 Fatty Acids EPA and DHA: Health Benefits Throughout Life. *Advances in Nutrition*, *3*(1), 1–7. https://doi.org/10.3945/an.111.000893

Teoh, M.-L., Phang, S.-M., & Chu, W.-L. (2013). Response of Antarctic, temperate, and tropical microalgae to temperature stress. *Journal of Applied Phycology*, *25*(1), 285–297. https://doi.org/10.1007/s10811-012-9863-8

Tinevez, J., Perry, N., Schindelin, J., Hoopes, G. M., Reynolds, G. D., Laplantine, E., Bednarek, S. Y., Shorte, S. L., & Eliceiri, K. W. (2017). TrackMate: An open and extensible platform for single-particle tracking. *Methods*, *115*, 80–90. https://doi.org/10.1016/j.ymeth.2016.09.016

Tiwari, A., Kiran, T., & Pandey, A. (2019). Chapter 14—Algal cultivation for biofuel production. In A. Basile & F. Dalena (Eds.), *Second and Third Generation of Feedstocks* (pp. 383–403). Elsevier. https://doi.org/10.1016/B978-0-12-815162-4.00014-8

TMR, T. M. R. (2016, September 21). *Global Algae Market is Projected to be Worth US$1.1 bn by 2024, at a CAGR of 7.39%; Global Industry Analysis, Size, Share, Growth, Trends, and Forecast 2016 - 2024: TMR*. Prnewswire. https://www.prnewswire.com/news-releases/global-algae-market-is-projected-to-be-worth-us11-bn-by-2024-at-a-cagr-of-739-global-industry-analysis-size-share-growth-trends-and-forecast-2016---2024-tmr-594253011.html

Tran, M., Hansen, J., Deaton, J., Wang, X., Gonzalez, O., Mayfield, M., & Mayfield, S. (2019). *High productivity methods for growing algae* (Canada Patent CA3082523A1). https://patents.google.com/patent/CA3082523A1/en?q=(triton+algae+inovations+chlamydomonas+miller+tran)&oq=triton+algae+inovations+chlamydomonas+miller+tran

Udayan, A., Pandey, A. K., Sirohi, R., Sreekumar, N., Sang, B.-I., Sim, S. J., Kim, S. H., & Pandey, A. (2023). Production of microalgae with high lipid content and their potential as sources of nutraceuticals. *Phytochemistry Reviews*, *22*(4), 833–860. https://doi.org/10.1007/s11101-021-09784-y

Varshney, P., Mikulic, P., Vonshak, A., Beardall, J., & Wangikar, P. P. (2015). Extremophilic micro-algae and their potential contribution in biotechnology. *Bioresource Technology*, *184*, 363–372. https://doi.org/10.1016/j.biortech.2014.11.040

Virtanen, O., Khorobrykh, S., & Tyystjärvi, E. (2021). Acclimation of Chlamydomonas reinhardtii to extremely strong light. *Photosynthesis Research*, *147*(1), 91–106. https://doi.org/10.1007/s11120-020-00802-2

Vishwakarma, R., Dhar, D. W., Jena, M., & Shukla, M. (2023). Pigment composition analysis of selected green microalgae through multivariate analysis and their potential as high value nutraceuticals. *Vegetos*, *36*(4), 1496–1508. https://doi.org/10.1007/s42535-022-00562-5

Walker, B. J., Abeel, T., Shea, T., Priest, M., Abouelliel, A., Sakthikumar, S., Cuomo, C. A., Zeng, Q., Wortman, J., Young, S. K., & Earl, A. M. (2014). Pilon: An Integrated Tool for Comprehensive Microbial Variant Detection and Genome Assembly Improvement. *PLOS ONE*, *9*(11), e112963. https://doi.org/10.1371/journal.pone.0112963

Winckelmann, D., Bleeke, F., Thomas, B., Elle, C., & Klöck, G. (2015). Open pond cultures of indigenous algae grown on non-arable land in an arid desert using wastewater. *International Aquatic Research*, *7*(3), 221–233. https://doi.org/10.1007/s40071-015-0107-9

Zdobnov, E. M., Kuznetsov, D., Tegenfeldt, F., Manni, M., Berkeley, M., & Kriventseva, E. V. (2021). OrthoDB in 2020: Evolutionary and functional annotations of orthologs. *Nucleic Acids Research*, *49*(D1), D389–D393. https://doi.org/10.1093/nar/gkaa1009

Zhang, B., Deng, C., Wang, S., Deng, Q., Chu, Y., Bai, Z., Huang, A., Zhang, Q., & He, Q. (2023). The RNA landscape of Dunaliella salina in response to short-term salt stress. *Frontiers in Plant Science*, *14*. https://doi.org/10.3389/fpls.2023.1278954

Zhang, C., Rabiee, M., Sayyari, E., & Mirarab, S. (2018). ASTRAL-III: Polynomial time species tree reconstruction from partially resolved gene trees. *BMC Bioinformatics*, *19*(6), 153. https://doi.org/10.1186/s12859-018-2129-y

Zhang, F., Li, Z., Duan, Y., Luan, H., Yin, L., Guo, Z., Chen, C., Xu, M., Gao, W., Fang, R. H., Zhang, L., & Wang, J. (2022). Extremophile-based biohybrid micromotors for biomedical operations in harsh acidic environments. *Science Advances*, *8*(51), eade6455.

https://doi.org/10.1126/sciadv.ade6455

Zheng, H.-Q., Chiang-Hsieh, Y.-F., Chien, C.-H., Hsu, B.-K. J., Liu, T.-L., Chen, C.-N. N., & Chang, W.-C. (2014). AlgaePath: Comprehensive analysis of metabolic pathways using transcript abundance data from next-generation sequencing in green algae. *BMC Genomics*, *15*(1), 196. https://doi.org/10.1186/1471-2164-15-196